Chinese Chemical Letters 34 (2023) 108336

Contents lists available at ScienceDirect

Chinese Chemical Letters

journal homepage: www.elsevier.com/locate/cclet

ROCK inhibitor: Focus on recent updates

Yaodong You[a,b,1], Kun Zhu[a,1], Jie Wang[c], Qi Liang[d], Wen Li[a], Lin Wang[e], Baojun Guo[a], Jing Zhou[a], Xuanlin Feng[f,*], Jianyou Shi[g,*]

[a] Hospital of Chengdu University of Traditional Chinese Medicine, Chengdu 610072, China
[b] TCM Regulating Metabolic Diseases Key Laboratory of Sichuan Province, Chengdu 610072, China
[c] Guizhou University of Traditional Chinese Medicine, Guiyang 550002, China
[d] College of Medicine, Southwest Jiaotong Unive, Chengdu 610031, China
[e] College of Food and Bioengineering, Xihua University, Chengdu 610039, China
[f] Department of Emergency Intensive Care Unit, Sichuan Academy of Medical Sciences & Sichuan Province People's Hospital, Chengdu 610072, China
[g] Department of Pharmacy, Personalized Drug Therapy Key Laboratory of Sichuan Province, Sichuan Academy of Medical Sciences & Sichuan Provincial People's Hospital, School of Medicine, University of Electronic Science and Technology, Chengdu 610072, China

ARTICLE INFO

Article history:
Received 5 January 2023
Revised 8 March 2023
Accepted 12 March 2023
Available online 15 March 2023

Keywords:
ROCK-I
ROCK-II
ROCK inhibitor
ROCK signaling pathway
Structure–activity relationship
Pharmacological activity

ABSTRACT

Rho-associated coiled-coil-containing protein kinase (ROCK) belongs to the serine-threonine family, and ROCK is involved in a variety of biological processes including cell migration, adhesion, proliferation and differentiation through phosphorylation of different downstream substrates. The aberrant activation of ROCK is associated with the pathological conditions in different systems including various diseases, including cancer, neurological diseases, inflammation, cardiovascular diseases and glaucoma. Therefore, the ROCK inhibitors have potential applicability for treating the aforementioned diseases. Four small molecule ROCK inhibitors have been approved for clinical use: fasudil, ripasudil, netarsudil and belumosudil. In recent years, more small molecule ROCK inhibitors have been identified. This paper reviews the ROCK inhibitors reported in past seven years. We mainly focused on the summarization of the structure–activity relationships, inhibitory efficacy, pharmacological mechanisms and the relevant clinical studies of the reported ROCK inhibitors. Besides the small molecular inhibitors, the peptides and biological extracts which exhibit ROCK inhibitory effects are also included. We also provide suggestions for the future development of the potent ROCK inhibitors.

1. Introduction

Rho is a Ras-related small guanosine triphosphate-binding protein (GTP-binding protein), which can be activated by guanine nucleotide exchange factors (GEF) as an active GTP-bound state. Rho-associated coiled-coil-containing protein kinase (ROCK) acts as downstream effectors of the small GTP-binding protein Rho [1,2].

GTP-bound form of Rho activates ROCK which further phosphorylate several downstream targets include myosin light chain (MLC), Rho-kinase inactivates myosin light chain (MLC) phosphatase (MLCP) through phosphorylating the myosin phosphatase targeting subunit 1 (MYPT1) at Ser696/Thr697/Ser854/Thr855, which leads to the enhancement of MLC phosphorylation. And some ROCK targets regulate in particular tissues, like formin homology 2 domain containing 3 (PHOD-3), which plays a vital role in sarcomere organization, myofibrillogenesis and maintenance of the contractile apparatus in cardiomyocytes [3]; the tubulin-associated unit has been associated with more than 25 neurological disorders, hyperphosphorylated and aggregated tau have been shown to increase the likelihood of cognitive impairments [4,5]. All these mechanisms have been summarized in Fig. S1 (Supporting information). ROCK mediates a wide range of biological processes including cell migration, adhesion, cytokinesis, cell proliferation, differentiation and apoptosis. Besides, ROCK also plays an essential role in neuropathies, cardiovascular disease, cancer development and inflammation. For example, ROCK directly phosphorylate phosphatase and tensin homolog (PTEN), therefore inhibit the growth and survival of tumor cells [6]. In addition, ROCK enhances endothelial function and neuroprotection through mediating elongation factor 1 alpha (EF-1α) [7]. The role of ROCK in controlling multiple biological events have made it an essential target for a variety of diseases. Hence ROCK inhibitors have received much attention in recent years. This review discusses some important

* Corresponding authors.
E-mail addresses: 23376592@qq.com (X. Feng), shijianyoude@126.com (J. Shi).
[1] These authors contributed equally to this work.

https://doi.org/10.1016/j.cclet.2023.108336
1001-8417/

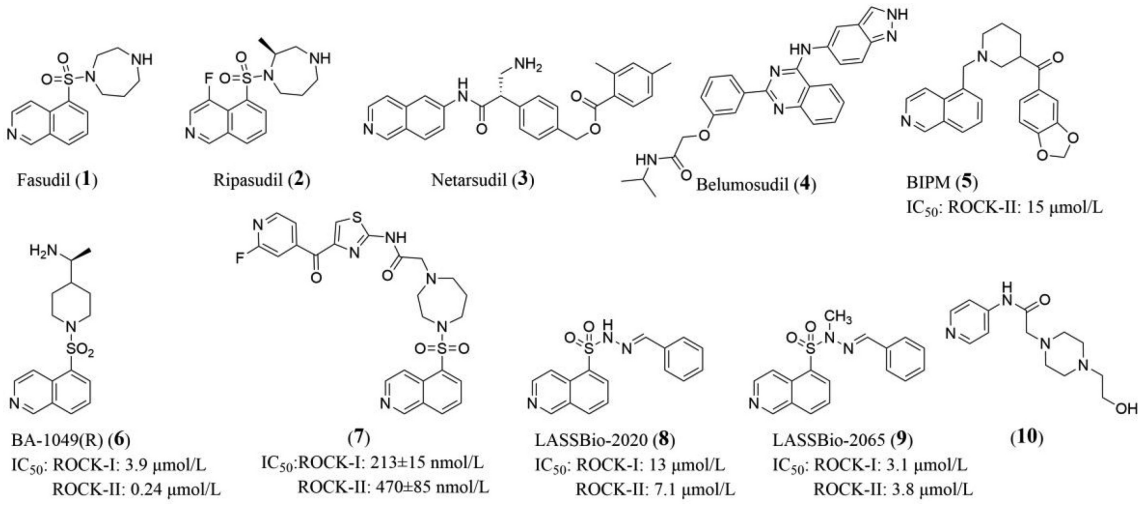

Fig. 1. ROCK inhibitors based on isoquinoline and pyridine/pyrrolopyridine derivatives.

structure–activity relationships (SAR), the binding patterns and design methods of ROCK inhibitors.

2. The development of ROCK inhibitors and the relevant clinical applications

The structural and expressive characteristics of ROCK are widely acknowledged (Text S1 in Supporting information). Given the high similarity of the structural domains between ROCK-I and ROCK-II kinases, both isoforms phosphorylate common substrates such as MLC, MYPT1 and LIMK to further regulate the actin-myosin cytoskeletal organization. In addition, both ROCK isoforms participate in the physiological processes of a variety of different systems including nervous, immune, and cardiovascular systems [8]. Besides modulate the cellular biomechanics through phosphorylation, ROCK also mediates gene regulatory signals. Combined with phosphorylated-STAT3 and regulating TH17/TFH gene transcription, ROCK-II regulates autoimmunity and inflammation [9]. ROCK also mediates the release of transcription factors, including myocardin-related transcription factor (MRTF), which indirectly modulates myocardial physiology [10]. Abnormal ROCK expression has been reported in multiple pathological conditions, including glaucoma [11], pancreatic cancer [12,13], gastric cancer [14], renal cell carcinoma [15], osteosarcoma [16], myocardial remodeling [17], aortic sclerosis [10,18], pulmonary arterial hypertension (PAH) [19], cognitive deficits [20], Parkinson's disease (PD), Alzheimer's disease (AD) [21,22], inflammation [18] and allergies [23]. Considering the role of the ROCK signaling pathway in oculopathy, neuropathies, cardiovascular disease, cancer, inflammation, human pluripotent stem cells, *etc.* ROCK targeting agents may potentially be exploited for treating the aforementioned diseases. Several drugs that specifically target ROCK are under development right now.

The primary approach to inhibiting the ROCK activity adopted by many investigators in the field is competing with type I adenosine triphosphate (ATP) in ROCK active conformation. Therefore, the ATP-binding pocket of the ROCK catalytic domain has been used as a basis for the development of small molecular inhibitors against ROCK [24].

The critical step in the development of ROCK inhibitors is to improve the binding affinity of the small molecule to the ATP-binding pocket of the ROCK catalytic domain. Considering the high similarity between ROCK-I and ROCK-II [25] and the similarity between ROCK and the closely homologous protein kinase A, G and C (AGC) kinase family, the inability of most ROCK inhibitors to specifically inhibit their targets may cause severe off-target effects [26–29]. Therefore, improving selectivity is another vital point for developing ROCK inhibitors.

Generally, the hit compounds are obtained *via* high-throughput screening (HTS) step, and then the functional groups are screened by SAR analysis for further optimization of the original compounds. Furthermore, in recent years, computer-aided drug design (CADD) has also been applied to predict the new inhibitor candidates [30]. The parameters CADD approach adopted include compound selectivity, toxicity and biological activity [31–34]. In particular, Sadybekov *et al.* [35] present the virtual synthon hierarchical enumeration screening (V-SYNTHES) approach, which rapidly detects the gigascale chemical spaces scoring the best-scoring lead. The team also apply V-SYNTHES on ROCK-I to predict small molecule compounds targeting ROCK-I, which yields a 28.5% hit rate, including ligands with nanomolar affinity and potency. The new method provides a practical alternative for rapidly screening the growing gigascale modular virtual libraries, helping to identify leads suitable for rapid optimization in the same REAL space.

3. Different categories of new ROCK inhibitors

Feng *et al.* [27] have reported more than 170 ROCK inhibitors and discussed their therapeutic potential before 2015. This review mainly summarized the new ROCK inhibitors identified in research papers in the last seven years (2016–2022). Here we categorize the ROCK inhibitors based on their hinge binding moieties. This review mainly focuses on SAR, selectivity, inhibitory efficacy, pharmacological mechanism and clinical research of small molecule compounds. We will also discuss classes of inhibitors that have not been reviewed before, such as natural plant extracts and peptides.

3.1. Classic ROCK inhibitors

Fasudil (**1**) (Fig. 1) was the first ROCK inhibitor approved for clinical use in Japan and China to treat vasospasms following subarachnoid hemorrhages. Since then, fasudil has been subsequently evaluated in acute ischemic stroke, angina pectoris, pulmonary hypertension, Raynaud's syndrome, arterial hypertension, neurodegeneration and glaucoma [36]. In 2014, ripasudil (**2**) (Fig. 1) has been approved for clinical use in Japan for the treatment of increased intraocular pressure in patients with glaucoma. In recent years, two new ROCK inhibitors were approved in the United States, netarsudil (**3**) (Fig. 1) in 2017 for treating hypertension and open-angle glaucoma, and belumosudil (**4**) (Fig. 1) in 2021 for

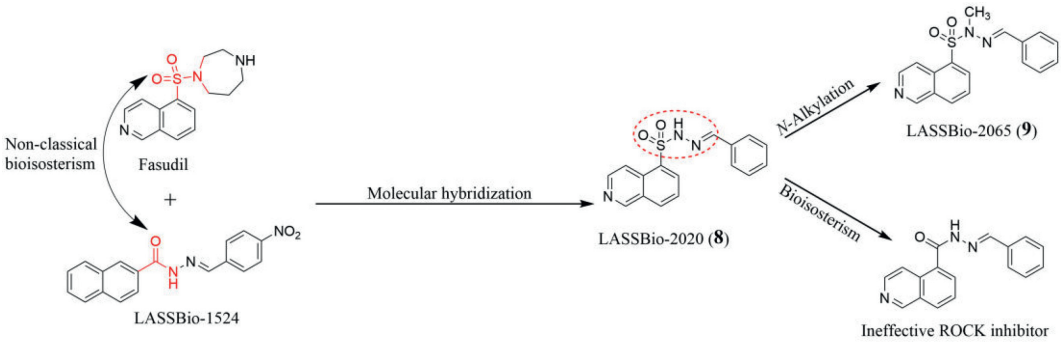

Fig. 2. Molecular hybridization to design ROCK inhibitors.

the treatment of graft-*versus*-host disease, idiopathic pulmonary fibrosis, liver disease and scleroderma. Ripasudil was developed by Kowa Co., Ltd., and fasudil was developed by Asahi Kasei, which were the first classical ROCK inhibitors, and both compounds are classical isoquinoline-based inhibitors. Another classical ROCK inhibitor is represented by Y27632, based on the 4-aminopyridine (and 4-aminopyrrolidine) scaffold, which is mentioned in the paper by Feng *et al.* [27].

Several derivative compounds based on the above classical inhibitor scaffolds have emerged recently. Some researchers have attempted to modify the substituent at the 5-position of isoquinoline to improve its inhibitory efficacy against ROCK. Chong *et al.* screened 1,3-benzodioxol-5-yl-[1-(isoquinolin-5-ylmethyl)piperidin-3-yl]methanone (BIPM) (**5**) (Fig. 1) as a potential ROCK-II inhibitor by docking and high-content drug screening [37]. The model analysis, kinase activity assay, and cell-based assays studied coherently confirmed that BIPM has ROCK-II inhibitory effects and is selective for focal adhesion kinase (FAK). The BIPM could promote neurite outgrowth; In SH-SY5Y cells (a human neuroblastoma cell line), BIPM could suppress cell migration, wound healing and stress fibers formation. Given that BIPM has no cytotoxicity to SH-SY5Y cells at concentrations ranging from 25 μmol/L to 100 μmol/L, it has been recognized as a promising inhibitor for anti-cancer treatments. Some investigators have made progress in molecular hybridization between fasudil and different scaffolds. The 5-substituted isoquinoline ring is essential for molecular recognition of the active site and is often preserved. BA-1049 (also known as NRL1049) is a racemic mixture designed by BioAxone BioSciences Inc (BBI) based upon fasudil structure [38]. The *R* enantiomer BA-1049 (R) (**6**) (Fig. 1) showed better selectivity for ROCK-II. BA-1049 (R) is 20–80 times more potent against ROCK-II [half-maximal inhibitory concentration (IC_{50}) = 0.24 μmol/L] than ROCK-I (IC_{50} = 3.9 μmol/L), and its metabolite 1-hydroxy-BA-1049 (R) showed better potency for ROCK-II. Both cellular and animal studies have demonstrated that BA-1049 (R) alleviates the symptoms of neurological diseases, disorders, and injuries in the tested models through oral or intravenous administration. In a follow-up study, the *Ccm1*$^{+/-}$ *Msh2*$^{-/-}$ and *Ccm3*$^{+/-}$ *Trp53*$^{-/-}$ mouse models with cavernous angioma (CA) lesions were selected for oral administration of the ROCK-II selective inhibitor BA-1049. The results showed BA-1049 slowed CA disease progression by decreasing non-hemoglobin deposition near lesions and reducing lesion growth and maturation. Besides, BA-1049 also exhibited little adverse reactions in the tested mice models that no dose-dependent wear and tear behaviors were observed even after four months of oral administration of 100 mg kg^{-1} day^{-1} [39]. BA-1049 is a promising selective inhibitor of ROCK-II for CA treatment.

Liang *et al.* [40] synthesized a series of fasudil-substituted thiazole compounds and screened out the ROCK-II inhibitor compound **7** (Fig. 1). SAR indicate that the pyridine-containing molecules showed higher ROCK inhibitory activity than other heterocyclic substituents, with the fluorine-substituted pyridine showing higher activity than the chlorine-substituted derivatives. Compound **7** showed significant cytotoxic activity against human breast cancer (MCF-7) cells (IC_{50} = 3.21 μmol/L) and was found more potent than fasudil (IC_{50} = 10.35 μmol/L). Cellular assays showed the inhibitory properties of compound **7** on the migration and invasion of MCF-7 cells. The *in vivo* pharmacological experiments results showed that compound **7** improved the body weight loss, reduced the oxidative stress in liver and mammary tissues, and improved intestinal function in the rat model with breast cancer.

Oliveira *et al.* designed a new family of *N*-sulfonyl hydrazide congeners by molecular hybridizing fasudil and the IKK-β inhibitor LASSBio-1524 (Fig. 2) [41]. The SAR indicate that the introduction of any substituent on the terminal benzene ring of *N*-sulphonylhydrazone derivatives leads to a reduction in the activity of the compound. Only the unsubstituted derivative LASSBio-2020 (**8**) (Fig. 1) showed better activity in inhibiting ROCK compare to the original two molecules with the IC_{50} values of 13 and 7.1 μmol/L for ROCK-I and ROCK-II, respectively [42]. Substituting an *N*-acylhydrazone group for the sulphonyl hydrazone group in LASSBio-2020 would result in an ineffective ROCK inhibitor. However, the *N*-alkylation of the *N*-sulphonylhydrazone moiety contributes to the bioactivity. The *N*-methylated analog LASSBio-2065 (**9**) (Fig. 1) was a slightly more potent ROCK inhibitor, which exhibited IC_{50} values of 3.1 and 3.8 μmol/L for ROCK-I and ROCK-II, respectively. The small difference in potency between these compounds may be because the *N*-methyl group in LASSBio-2065 rotates the N-S bond, which allows the compound to have extra hydrophobic interaction with Leu205. This interaction was not seen in LASSBio-2020. Neither of these compounds inhibited IKK-β at a screening concentration of 10 μmol/L, and both derivatives LASSBio-2020 and LASSBio-2065 effectively inhibited cell migration in cell-based assays. In addition, no cytotoxicity was observed for these compounds in serum lactate dehydrogenase (LDH) and 3-(4,5-dimethyl-2-thiazyl)-2,5-diphenyl-2*H*-tetrazolium bromide (MTT) assays.

Another class of classical ROCK inhibitors is compounds designed based upon aminopyridine scaffolds by Yoshitomi Pharmaceutical [43,44]. As an antagonist of voltage-gated potassium (Kv) channels, 4-aminopyridine (4-AP) is used as symptomatic therapy in several neurologic disorders [45]. Based on the mother nucleus 4-AP, Li *et al.* synthesized five novel 4-AP derivatives as neuroprotective agents. Three compounds exhibited ROCK inhibitory activity [46].

Among these, compound **10** (Fig. 1) exhibited the most favorable properties compared to the other two. The docking result shows that the hydrogen bond formed between the pyridine ring and hydroxyl in compound **10** and Met156 in ROCK-II, and Met172

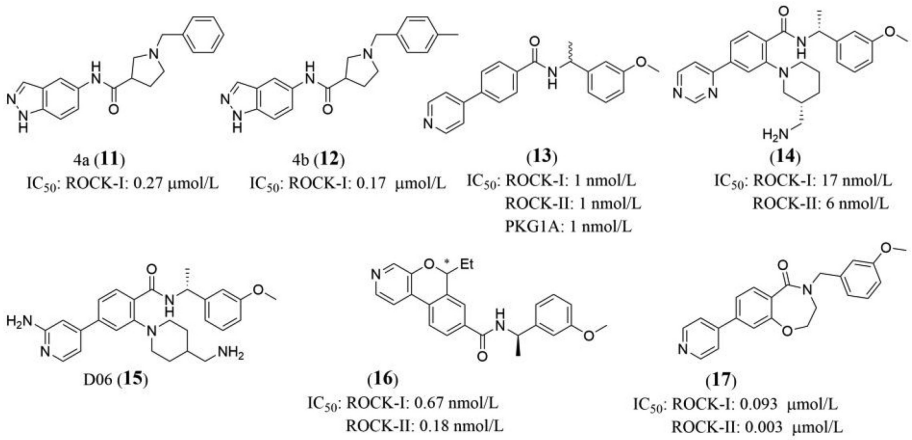

Fig. 3. Indazole, pyridine, and pyrimidine based ROCK inhibitors.

in ROCK-II is the key to the binding possibility. The docking result also indicates that the affinity of this 4-AP derivative for ROCK is similar to that of fasudil. The hydroxyl group on compound **10** effectively enhances the expression of heme oxygenase-1 (HO-1) (a stress-inducible and redox-sensitive protein) and also enhances the ROCK potency of compound **10**. Cellular assays have shown that compound **10** effectively inhibits the expression of α-synuclein, exhibiting potential neuroprotective effects, and it also shows some antioxidant and anti-inflammatory properties [46].

3.2. Indazole based ROCK inhibitors

The indazole derivatives developed as ROCK inhibitors in the late 1990s and early 2000s. The indazole portion of these compounds serves as a hinge binder. Yao *et al.* reported the design, synthesis and SAR studies of a series of novel *N*-substituted prolinamido indazoles as ROCK-I inhibitors [47]. The investigators reported a ROCK-I inhibitor, 5-nitro-1*H*-indazole-3-carbonitrile (DL0805) (Fig. S3 in Supporting information), in the previous literature [48]. The series III (Fig. S3) compounds were synthesized by selecting the flexible *N*-substituted proline amino group containing the benzyl substituent to replace the NO_2 group at the 5-position of the indazole of DL0805, and this series exhibited the best inhibitory activity. The 4-position substituent of the terminal benzene ring affects the activity of the compounds in the following order: CH_3 > H > Br > OCH_3> F> NO_2, CN (Fig. S3). Compounds **11** and **12** (Fig. 3) exhibited potent ROCK-I inhibitory activity with IC_{50} values of 0.27 and 0.17 μmol/L respectively. The *in vivo* experiments results demonstrated that **11** and **12** have vasodilatory activity in rat aortic rings comparable to that of the clinically approved drug fasudil. The potent active compound **12** (also named DL0805-2) with superior activity was further evaluated to prevent angiotensin II (Ang II)-induced vasoconstriction by inhibiting Ang II-induced intracellular Ca^{2+} elevation and ROCK pathway activation under *in vitro* conditions [49].

3.3. 4-Carboxamido-aromatic ring substituted-pyridine, pyrimidine based ROCK inhibitors

This class of compounds form hydrogen bonds with ROCK mainly through the nitrogen in the pyridine and the amide carbonyl, respectively. Based on the HTS results, Hobson *et al.* [50] identified a series of potent and kinome-selective dual ROCK-I and ROCK-II inhibitors. The experiment results demonstrate the compounds **13** and **14** (Fig. 3) are excellent dual ROCK-I and ROCK-II inhibitors. The interrogation of the co-crystal structures indicated that, compounds with the (*R*) configuration at the benzylic carbon were more effective than those with the (*S*) configuration as ROCK inhibitor. Compound **13** was shown to be a potent dual inhibitor of ROCK-I and ROCK-II in enzymatic and cellular assays, with an IC_{50} value of 1 nmol/L for ROCK-I/II. However, extensive kinome analysis showed compound **13** inhibited two other kinases at the low nanomolar level, PKG1A (IC_{50} = 1 nmol/L) and PKA (IC_{50} = 47 nmol/L). Furthermore, compound **13** protects the axons in the retinal nerve fiber layer after oral dosing. Compound **13** may be considered a mother molecule for further studies of developing bifunctional inhibitors. As shown in Fig. S4 (Supporting information), the substitution of the hinge part from pyridine to pyrimidine and the introduction of piperidine-3-ylmethanamine from the *meta* position of the central aryl ring (R_1 group) improved the selectivity profile for ROCK-I and ROCK-II inhibitors, which led to compound **14**. The substitution of R_2 with a propyloxy group was not conducive to identifying ROCK-I and ROCK-II inhibitors, but that of the methoxy group resulted in increased activity. The pyrimidine substitution gave compounds afforded a clean cytochrome P450 (CYP) inhibition profile. In addition, the group explored the effects of different hinge binding motifs on polar surface area (PSA) and fraction sp^3 carbon (Fsp^3). Piperidine increased the PSA and Fsp^3 values associated with a safer predicted toxicity profile rather than 2-aminopyridine, 2-fluoropyridine, and 3-fluoropyridine. Compound **14** was shown to be an excellent and selective dual ROCK-I and ROCK-II inhibitor with IC_{50} value of 0.094 μmol/L in the pMYPT1 enzyme-linked immunosorbent assay (ELISA) cell assay. This compound has excellent predicted drug-like properties, including a significantly reduced CYP inhibition profile [50].

CADD also contributes to the development of new ROCK inhibitors [32,34,35]. Ghosh *et al.* [31] analyzed the ROCK inhibitors proposed by Hobson *et al.* [50] using a prediction models established by approaches include docking, molecular dynamics, and three-dimensional quantitative structure–activity relationships (3D-QSAR). Based upon the aforementioned analysis, 40 pyridinylbenzamide-based ROCK-I inhibitors were designed in silico. The biological activities of the designed molecules were also analyzed using the same prediction models and seven lead compounds of ROCK-I inhibitors (D02, D03, D06, D31, D32, D33, D35) were selected from them. In this study, the IC_{50} values, which were in μmol/L units, were converted to log IC_{50} (pIC_{50}) values. The predicted pIC_{50} values of all seven compounds were around 8; for example, compound D06 (**15**) (Fig. 3) with pIC_{50} value of 8.58. Although absorption distribution metabolism excretion toxicity (ADME/Tox) and synthetic accessibility (SA) score analysis indicate that these compounds have desirable pharmacokinetics (PK)

property and bioavailability, investigators still need to synthesize the compounds and verify the relevant parameters with both *in vitro* and *in vivo* experiments.

Through kinase screening, Bristol-Myers Squibb (BMS) reported a series of 5*H*-chromeno[3,4-c]pyridine, 6*H*-isochromeno[3,4-c]pyridine, and 6*H*-isochromeno[4,3-d]pyrimidine based dual ROCK-I and ROCK-II inhibitors and compound **16** (Fig. 3) was screened among them [51]. The SAR analysis indicate that the replacement of the ether with a benzamide linker lead to moderate improvement in ROCK inhibition potency. The introduction of a *meta*-methoxy substitution on the phenyl or a benzylic methyl substitution improved the molecule's ROCK-II inhibitory potency (IC_{50} value) further to single-digit nanomolar level. Compared to C5-methyl substitutions, C6-methyl/ethyl substitutions on the central ring could potentially improve its ROCK-II inhibitory potency (Fig. S5 in Supporting information). The diastereomer compound **16** exhibits sub-nanomolar ROCK-I and ROCK-II IC_{50} potencies (0.67 and 0.18 nmol/L, respectively) with outstanding kinome selectivity.

In some structures, the amido nitrogen is ring-closure to the central phenyl ring. Sun *et al.* performed structural optimization and SAR analysis on three regions of the scaffold 3,4-dihydroisoquinolin-1(2*H*)-one and reported a series of 3,4-dihydrobenzo[*f*][1,4]oxazepin-5(2*H*)-one derivative [52]. The most active compound, **17** (Fig. 3), was obtained by replacing 3,4-dihydroisoquinolin-1(2*H*)-one moiety, 1*H*-indazole molecule with 3,4-dihydrobenzo[*f*][1,4]oxazepin-5(2*H*)-one, and 4-pyridine groups, respectively, which had the highest activity against ROCK-I and ROCK-II ($IC_{50} = 0.093$ and 0.003 μmol/L, respectively). The crystal structural analysis of the compound **17** and ROCK-I/II complexes confirmed that there are two hydrogen bonds formed between **17** and ROCK-I: the nitrogen of pyridine and Met156 and the amide carbonyl with Lys105. Three hydrogen bonds formed between **17** and ROCK-II: the nitrogen of pyridine and Met172, the amide carbonyl and Lys121, and the 3-methoxy oxygen atom with Lys216. This explained why **17** exhibits a higher inhibitory activity against ROCK-II than ROCK-I. At a fixed concentration of 10 μmol/L, **17** exhibited higher inhibition only against LIMK2. What is more, the *in vivo* experiment results showed **17** rapidly and significantly lowers the intraocular pressure (IOP), and no evident hyperemia was observed during the experiment in the normotensive New Zealand rabbits. But as a lead compound, further refined and in-depth studies are necessary to obtain more effective ROCK inhibitors.

3.4. 4-Amido (urea or carbamate)-aromatic ring substituted-pyridine, pyrrolopyridine based ROCK inhibitors

For pyridine derivatives, 4-pyridine derivatives are usually more effective as ROCK inhibitors than 3-pyridine derivatives. Usually, the introduction of side chain solubilizing groups not only enhances potency and selectivity but also increases the solubility of the compounds [53–55].

Recently, a series of potent and selective ROCK-II inhibitors based on 4-aryl-5-aminoalkyl-thiazole-2-amines was reported by Ma and Wang *et al.* [56,57]. SAR of this series of compounds have been summarized as follows: Firstly, the substitution of the acid moiety (R_1 group) with a pyridine group was not conducive to identifying target inhibitors, but that of 2,3-dihydrobenzo[*b*][1,4] dioxin group substitution resulted in higher activity. Secondly, compounds with a morpholine group substituent at the aminoalkyl side chain (R_2 group) enhanced anti-ROCK-II enzyme activity more than compounds with other groups, such as dimethylamine, *N*-methyl piperazine, *N*-methyl-*N*-iso-propylamine, piperidine, and pyrrolidine. Thirdly, it seems that the basic tertiary amine group in the side chain was beneficial to the ROCK-II inhibitory activity (Fig. S6 in Supporting information). The most effective inhibitor against ROCK-II is **18** (Fig. 4) ($IC_{50} = 0.02$ μmol/L). Molecular docking of compound **18** with ROCK-II indicated two key hydrogen-bond interactions between the nitrogen in the pyridine ring with Met172 and Lys121. More experiments are needed to further verify and disclose more SAR features of the pyridine and pyrrolopyridine based ROCK inhibitors.

Based on the compound **18** [56], to improve its inhibitory potency and selectivity, Wang *et al.* designed 24 new chemical entities as the lead compounds of ROCK inhibitors. They found some active urea-like compounds using the splicing and bioisosteric isometric method [58]. Among them, compound **19** (Fig. 4) is the most potent inhibitor of ROCK-I and ROCK-II, with IC_{50} values of 1.1 and 0.03 μmol/L, respectively. The SAR analysis indicated that the pyrrolidine groups in compound **19** enhanced the ROCK inhibition. The previous studies have shown that the hinge binder of pyridinethiazole urea-based ROCK inhibitors is the pyridine ring nitrogen. The nitrogen atom of pyridine formed one H-bonding interaction with the main chain amide NH of Met156 [59]. However, considering the small molecular PSA of compound **19** and the short dialkyl aminomethyl side chain, it only forms an H-bond with Lys216 through the pyridine ring nitrogen. In addition, the authors disclosed the azaindole group scaffold **20** (Fig. 4), which demonstrated a selectivity ratio of 118 for ROCK-II inhibition, making it the most selective inhibitor among the compounds studied [58].

Based on the previous well-known ROCK inhibitor benzodioxane 3′-carboxamide SR3677 [60,61], the Scripps Research Institute has developed a potent and enantiomer-selective ROCK-II inhibitor [62]. SAR analysis indicated that substituting the pyridine group with a hinge-binding molecule and substituting the C6 position (R group) of the tryptophan ring with with a 6-methoxy group reduces inhibition of ROCK-I while maintaining activity against ROCK-II. This compound exists in both *R* and *S* conformations, and (*S*)-7c (*S*-configuration of this compound) (**21**) (Fig. 4) showed better ROCK inhibitory activity ($IC_{50} = 170$ nmol/L against ROCK-I and 9 nmol/L against ROCK-II). Molecular docking analysis showed that both the *R* and *S* conformations form the same hydrogen bond with ROCK-II: the amide carbonyl with Lys121 (critical for isomer selectivity), protonated $(CH_3)_2N$ with Asp176, pyridine nitrogen with Met172. The seven hydrophobic rings in the **21**-ROCK-II complex (Met169, Leu221, Val106-C···pyridine ring; Lys121-C-pyran ring; Leu123-C, Phe136···phenyl ring of chroman) explain why **21** showed better ROCK-II inhibition and isomer selectivity (Fig. 5). However, the authors did not report the PK parameters of compound **21** *in vitro* or *in vivo*.

Vertex Pharmaceuticals Incorporated (VPI) has synthesized a series of *N*-acylated aminothiazoles and *N*-acylated aminothiophene and evaluated their biological activity against Rho kinase [63]. The X-ray crystal structure indicated that the substitution of the central thiazole or thiophene ring is the most suitable of all five- or six-membered rings to increase the inhibitory potency of ROCK. Extending the substituent into the pocket defined by the glycine-rich loop enhanced ROCK-I inhibition potency. Compound bearing a 3-methane-sulfonyl amino group provided the best overall combination of potency and selectivity. In addition, the 2-fluoro-substituted pyridine effectively reduces CYP inhibition while maintaining good ROCK-I potency and PKA selectivity (Fig. 6). Compound **22** (Fig. 4) was able to inhibit the enzymatic activities of ROCK-I ($IC_{50} = 10$ nmol/L) with 300-fold selectivity against PKA, desirable selectivity against a panel of kinases, good cellular potency, and excellent PK profiles [63].

To enhance the solubility and target potency and selectivity against PKA of ROCK inhibitors, VPI introduced a solubilizing side chain at the 3-position of phenylethylamide in the previously reported *N*-acylated aminothiazole compound **a** (Fig. 6)

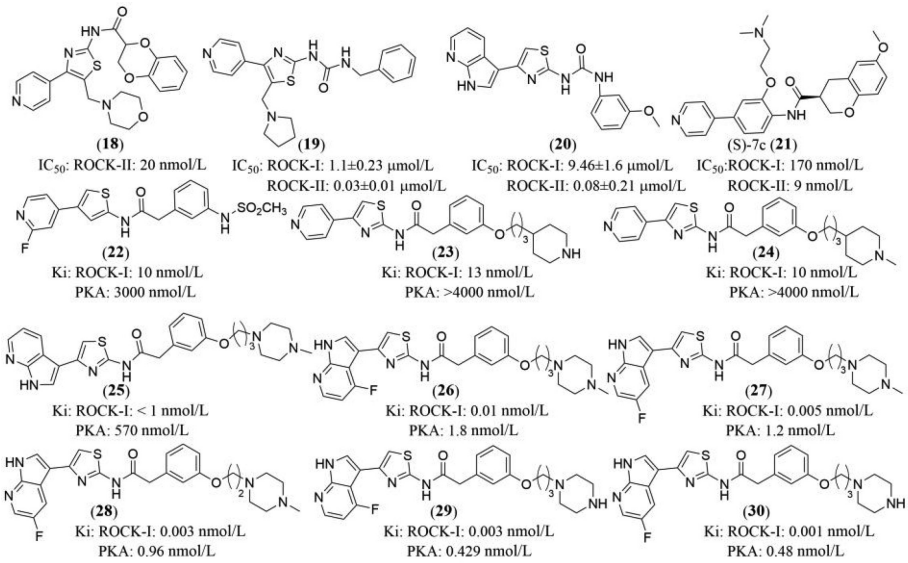

Fig. 4. Pyridine and pyrrolopyridine based ROCK inhibitors.

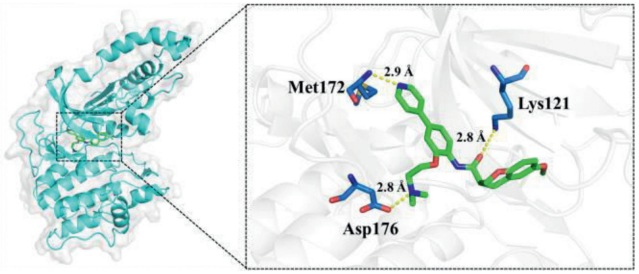

Fig. 5. Crystal structure of **21** complexed with the kinase domain of ROCK-II (PDB ID: 4L6Q). The crystal structure of **21** (green) bound to the active site of ROCK-II. Hydrogen bonds are shown as dashed lines.

[53,63]. SAR analysis indicated that the best solubilizing group was solubilized piperidine or piperazine linked by a 3-carbon linker, which resulted in solubility values > 200 μmol/L for this class of compounds (Fig. 6). Modeling and X-ray crystallographic analysis showed that the inhibitors with additional solubilizing groups bind to Asp117 of ROCK, providing additional interactions [53]. Piperidine derivatives with nitrogen atoms at the end of the molecule, such as compounds **23** and **24** (Fig. 4), exhibited the best ROCK inhibition. In contrast, compound **23** showed no significant inhibition towards the 20 kinases tested (all IC_{50} values >1 μmol/L) [53].

VPI modified the 2-amino substituent of *N*-acylated aminothiazoles compound **b** (Fig. 6) to a 4-substituted 7-azaindole ring and reported a highly potent and PKA selective series 7-azaindole-based ROCK inhibitors [54]. The best compounds reported were shown to have a high ROCK potency with K_i values in the single-digit nanomolar level; for example, compound **25** (Fig. 4) demonstrated a greater ROCK-I inhibition with K_i <1 nmol/L [54]. SAR indicated that 3-substituted 7-azaindole substitution enhances the ROCK potency (Fig. 6). X-ray crystal structure indicated that the lowest energy state for compounds occurs when the biaryl from the 4-position is shifted to the 3-position of 7-azaindole, and thiazole and azaindole rings are coplanar. The 3-substituted 7-azaindoles maintain the same ROCK inhibitory effect and the corresponding hydrogen bond, indicating that the 3-substituted 7-azaindoles are bioisosteric replacements for 4-

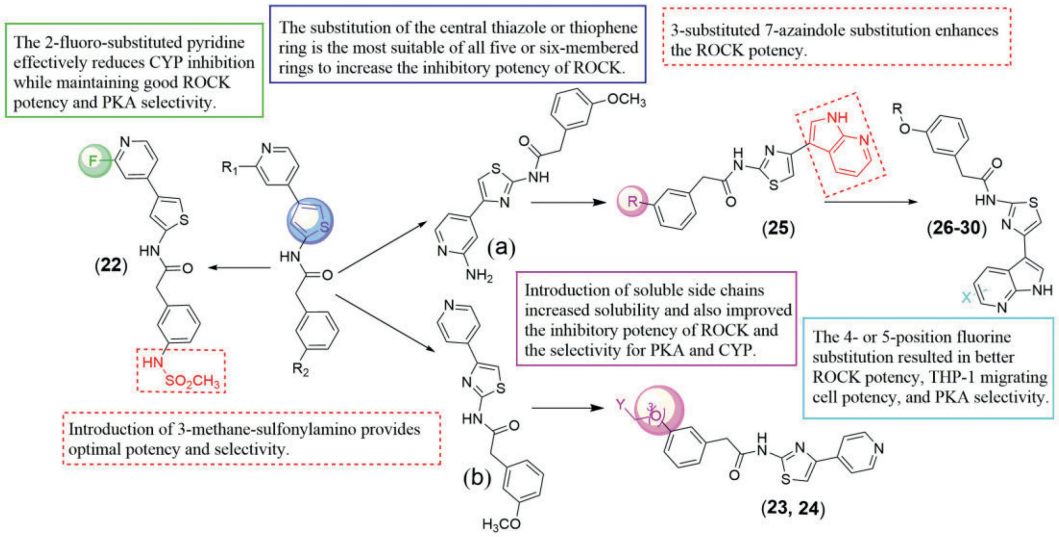

Fig. 6. Structure–activity diagram of **22**–**30**.

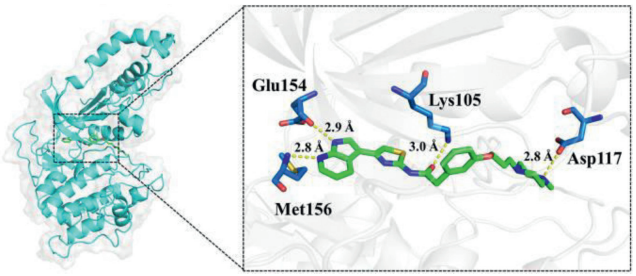

Fig. 7. Crystal structure of compound **25** complexed with the kinase domain of ROCK-I (PDB ID: 5KKT). The crystal structure of compound **25** (green) bound to the active site of ROCK-I. Hydrogen bonds are shown as dashed lines.

substituted pyridines. The 3-substituted 7-azaindole compounds form three hydrogen bonds between the 7-azaindole nitrogen and Met156, azaindole pyrrole NH and backbone carbonyl of Glu154, the backbone NH and Lys105. Furthermore, the addition of the solubilizing group piperazine N-Me, which interacts with Asp117, improves the ROCK inhibition potency and selectivity for PKA and CYP (Fig. 7).

VPI next explored 7-azaindole substituents at the 4- and 5-positions with fluorine, chlorine, bromine, and hydroxyl. Moreover, VPI designed a series of ROCK-I inhibitors (compounds **26**–**30**) (Fig. 4) that exhibited excellent ROCK potency. Compound **30** showed the highest PKA selectivity (> 480-fold) while maintaining excellent ROCK-I potency ($K_i = 0.001$ nmol/L) [55]. SAR analysis indicated that the central thiazole ring substitution was more effective than substitutions with other five- or six-membered rings in enhancing ROCK inhibition potency. The 4- or 5-position fluorine substitution resulted in better ROCK potency, human monocytic leukemia cell (THP-1) migrating cell potency, and PKA selectivity (Fig. 6). *In vivo* rat PK profiling indicated that compounds substituted with solubilizing chains for the R group exhibited higher plasma clearance (>65), higher volume of distribution (>10), and longer $T_{1/2}$ (>3 h).

3.5. 4-Amido-aromatic ring substituted-pyrazole based ROCK inhibitors

BMS scientists have identified a series of novel phenylpyrazole amide derivatives through internal kinase data mining, rational design, and SAR analysis [64]. The pyrazole part of the molecule is considered to be the hinge binder. Compound **31** (Fig. 8) was discovered to be a potent dual ROCK-I/II inhibitor. The introduction of butylbenzene with a polar group (amino) to the aniline amide structure effectively improved metabolic stability, solubility, and inhibition of ROCK. Among the identified phenylpyrazole amide derivatives, the compound **31** has a balanced kinome selectivity (value 6/261) and a half-life value of 41 min for human liver microsome (HML) metabolic stability. Furthermore, compound **31** demonstrated good PK profiles with C_{max} 28 nmol/L, AUC of 140 nmol/L*h. The Parallel artificial membrane permeation assay (PAMPA) value was 450 nm/740 sec at pH 5.5 and 7.4. Also, the *in vivo* experiments results indicate that the antihypertensive effect of compound **31** is dose-dependent.

3.6. Thieno[2,3-d]pyrimidin-4(3H)-one, benzothiophene substituted pyridine (pyrimidine, pyrrolopyridine) derivatives as ROCK inhibitors

Miao *et al.* discovered a hit compound based on molecular docking virtual screening (VS) approach [65]. The relevant structural optimization and SAR evaluation were performed based on the hit compound (Fig. S7 in Supporting information). The SAR analysis demonstrate the thieno[2,3-*d*]pyrimidin-4(3*H*)-one moiety is the optimal fragment in region I, which made the compound exhibit a significant improvement in ROCK inhibitory potency. Region III was fixed in its original form, as the other substituted phenyl groups of region III could not improve the compound's activity. The substitution of region II showed that the introduction of either the pyridine group or 7-azaindole enhanced the ROCK inhibitory activity, but 7-azaindole was the best choice for region II. The most representative compound **32** (Fig. 8) displayed IC_{50} values against ROCK-I and ROCK-II of 0.004 and 0.001 μmol/L, respectively. The *in vitro* experiments showed compound **32** effectively changed cell shape, prevented cell migration and inhibited ROCK activity in intact cells.

Benzothiazole-substituted pyridine derivatives as ROCK inhibitor scaffolds are more classical [66]. Judge *et al.* synthesized a series of 2-aminobenzothiazole-like inhibitors of ROCK-I/II based on molecular docking and SAR approaches [67]. The investigators tried to introduce the benzylamine group to benzothiazole. The crystal structures of compound-ROCK complexes indicated that (*R*)-configuration benzyl moiety in these compounds is sandwiched by hydrophobic interactions between phenylalanine 55, lysine 73, and the flexible glycine-rich loop of the kinase. Such interaction often plays a large role in potency and kinase selectivity. Therefore, the (*R*)-configuration is the preferred stereochemistry at the benzyl carbon of these compounds. As a result, compound **33** (Fig. 8) was obtained. The phenyl group at the end of **33** contributes to its activity, and the introduction of *N*-methyl-*N*-(3-methylbutyl)methanamide at the phenyl 3-position afforded compound **34** (Fig. 8) and a slight decrease in ROCK inhibition was observed, but the selectivity was greatly enhanced. Although some compounds exhibited higher ROCK inhibition by compound modification, only compounds **33** and **34** showed the cleanest kinome profiles. In cellular assays, both compounds showed submicromolar activity and exhibited a role as ROCK inhibitors in pain management. In a model of chronic constriction injury of the sciatic nerve, compound **33** exhibited the same efficacy as fasudil.

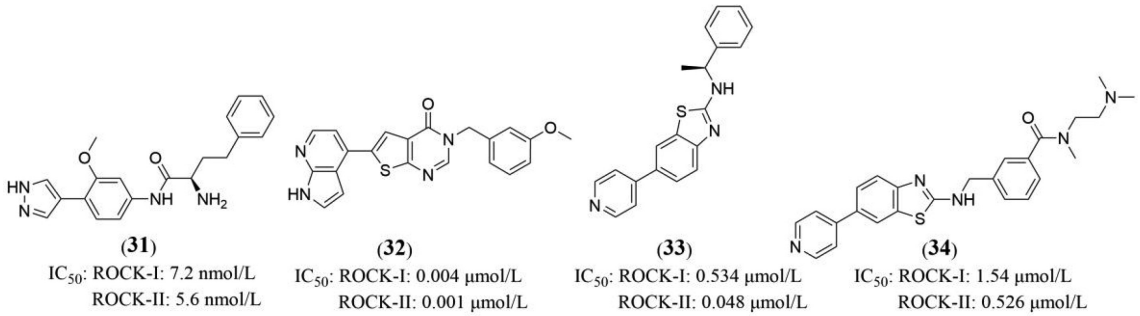

Fig. 8. Pyrazole, thiophene substituted pyrrolopyridine, and benzothiophene substituted pyridine based ROCK inhibitors.

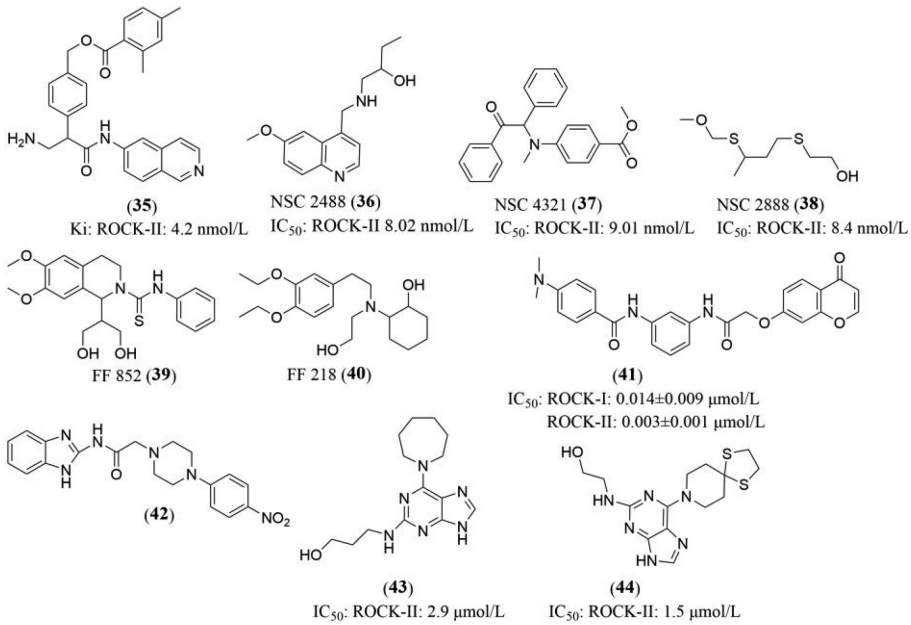

Fig. 9. 6- and 7-substituted isoquinoline, 4-chromanone, benzimidazole, purine derivatives as ROCK inhibitors.

3.7. 6-/7-Isoquinoline, 4-chromanone, benzimidazole, naphthalene, purine derivatives as ROCK inhibitors

Some of the ROCK inhibitors are derivatives based on the bicyclic aromatic ring ([6,5]- and [6,6]-fused rings) scaffolds. Previous studies showed that the potent ROCK inhibitors with good enzymatic and cellular potency can be developed by attaching aryl or heterocyclic portions (*e.g.*, pyrazoles, amino pyrimidines) to bicyclic aromatic ring scaffolds using appropriate linkers [65,67], such as the benzimidazole-substituted pyrazole scaffolds [68,69]. Unlike the pyrazole or aminopyrimidine ROCK inhibitors with a bicyclic aromatic ring as the central part, the following compounds are all bicyclic aromatic ring derivatives.

AR-12286 is a ROCK inhibitor developed by Aerie Pharmaceuticals, but it failed to pass the phase II clinical trial [70,71]. Aerie described the discovery of novel amino-isoquinoline amide ROCK inhibitors that provide a longer duration of IOP-lowering effect in animal models than AR-12286 [72]. The 2,4-dimethyl benzoate analog **35** (Fig. 9) is the most effective compound obtained by a series of modifications based on AR-12286. First, the introduction of the α-aryl-β-amino group at the aminoalkyl arm of AR-12286 then substituted with hydroxymethyl at the 4-position of the α-aryl ring. To reduce the hyperemia and improve corneal penetration, the group prepared esters of the 4-hydroxymethyl fraction. These modifications greatly enhanced the inhibitory effect on ROCK. Specifically, the α-aryl-β-amino derivative exhibited significant improvement of ROCK potency in both human trabecular meshwork (HTM) and primary porcine trabecular meshwork (PTM) cell assays. Compound **35** significantly lowers its IOP sustainably and producing only mild hyperemia with no chemosis. The introduction of the α-aryl-β-amino portion mentioned earlier resulted in compound **35** have both (*S*) and (*R*) enantiomers. The *S*-enantiomer has better activity, and continued studies on compound **35** led to the discovery of the *S*-enantiomer, netarsudil [73].

Hsu *et al.* reported an aminoisoquinoline derivative, ITRI-E-212 (structure not disclosed), could reduce IOP by increasing the water flow through the trabecular meshwork [74]. ITRI-E-212 exhibited an IC_{50} of 0.25 μmol/L for ROCK-II. ITRI-E-212 effectively penetrates the cornea and maintains ROCK-II inhibitory activity in the aqueous humor. In a normotensive rabbit model, nearly 25% of the peak percentage change in IOP was observed within 4 h after administration of 1.0% ITRI-E-212 eye drops. In a hypertensive rabbit model, IOP was reduced by 28.6% after 6 h of administration of 1.0% ITRI-E-212 drops. In this study, 1.0% ITRI-E-212 maintained low IOP for at least 6 h with only transient mild conjunctival congestion following a once-daily dosing regimen. The drug still needs further human trials.

ITRI-E-247 (structure not disclosed) is a highly selective and potent ROCK inhibitor reported by Tu *et al.* in 2019. This agent inhibits MLC phosphorylation in a concentration-dependent manner and causes cell relaxation in vascular smooth muscle cells (A7r5 cells). In rabbits, 0.5% ITRI-E-247 drops significantly reduced IOP by 32% at the time point of 6 hours post topical drops with no severe ocular toxicity observed. No information is available regarding its use in clinical trials [75].

Kesar *et al.* reported a series of ROCK inhibitors developed based on pharmacological models [76]. This pharmacological model contains four basic chemical features: hydrogen-bond acceptor (HBA), hydrogen bond donor (HBD) and hydrophobic agent (HY). NSC 2488 (**36**) (Fig. 9) exhibited the highest inhibitory potential ($IC_{50} = 8.02$ nmol/L) and showed comparable potency to Y-27632. The molecular interactions between the functional groups of NSC 2488 and the active site amino acids of the ROCK-II protein structure are summarized as follows. The nitro group of 6-methoxyquinolin-4-yl showed hydrogen bonding with GLY104. The methyl group interacts with Lys121 and Phe103 through van der Waals force and the hydroxyl group of 2-butanol interacts with Gly234 through van der Waals force too. In addition, Asn219, Asp232, Met169, Ala119 and Val106 formed a hydrophobic environment around NSC 2488. Kesar *et al.* synthesized two new ROCK inhibitors NSC 4231 (**37**) and NSC 2888 (**38**) (Fig. 9) with IC_{50} values of 9.01 and 8.4 nmol/L which are based upon the same pharmacophore as NSC 2488. *Ex vivo* experiments results revealed that all three compounds exhibited concentration-dependent relaxation and vasodilatory activity similar to standard Y-27632. The Tanimoto similarity index for the three compounds was 0.08, 0.12 and 0.13 (<0.5), respectively, indicating all three are novel compounds.

Different from 6-amino-substituted isoquinoline derivatives, Domokos *et al.* synthesized the ROCK inhibitor FF 852 (**39**) (Fig. 9) through linkage dialkoxy to the 6- and 7-positions of the tetrahy-

droisoquinoline core. The replacement of the tetrahydroisoquinoline with a benzene ring resulted in the synthesis of FF 218 (**40**) (Fig. 9). FF 852 and FF 218 relax uterine smooth muscle in pregnant rats. Furthermore, FF 852 and FF 218 relax the uterus during parturition (when ROCK expression was high) in rats with greater potency than fasudil [77].

Zhao *et al.* reported a series of new ROCK inhibitors based on the 4*H*-chromen-4-one core. [78]. Among which, the compound **41** (Fig. 9) is the most representative potent and kinome-selective dual ROCK-I and ROCK-II inhibitor. Compound **41** form four hydrogen bonds with ROCK-II. Among them, the carbamoyl group flanked by the intermediate group formed three hydrogen bonds with ROCK-II residues Phe103, Asp232 and Lys121. In addition, the carbonyl of the chromone forms a hydrogen bond with residue Met172, and this bond is very important for stabilizing the orientation and conformation of **41**. The *in vitro* assays results showed compound **41** prevents endothelial cell migration and rescues neurons from high glucose-induced injury. In retinal explants, compound **41** effectively reduced high glucose-induced Müller glial growth. In general, compound **41** is promising for diabetic retinopathy (DR) treatment.

Several studies have demonstrated that benzimidazole substituted pyrazole and piperazine groups are the active structural components of many ROCK inhibitors [68,69,79]. By linking a piperazine moiety to the benzimidazole scaffold with a hydrophobic linker, many hydrophobic interactions arise with the ROCK hydrophobic P-loop. A series of benzimidazole derivatives containing acetamide-linked substituted piperazines were designed and synthesized by Abbhi *et al.* [80]. Compound **42** (Fig. 9) containing *p*-nitrophenyl substituted piperazine showed good ROCK-II inhibitory activity. Compound **42** inhibited ROCK-II enzymes at a rate similar to that of fasudil. The inhibition of ROCK-II by compound **42** at a concentration of 0.5 and 1 mmol/L was 57.25% and 77.92%, respectively. Molecular docking analysis revealed there are two hydrogen bonding links between ROCK-II and compound **42**: the carbonyl oxygen of the acetamide and Lys121, the nitrogen of the acetamide linker, and Ala231. The acetamido portion of the compound increased its lipophilicity and promoted corneal permeation. The percentage reduction in IOP at peak effect (2.5 h after administration) of compound **42** was 51.56%. In the 2,2-diphenyl-1-picrylhydrazyl (DPPH) radical scavenging assay, compound **42** had an IC_{50} value of 95.49 mg/mL, indicating that it has significant antioxidant potential and may protect neurons from oxidative stress. Because oxidative free radicals damage neuronal cells and cause optic nerve damage, ROCK inhibition combined with the targeting oxidative free radicals is an effective therapeutic route for glaucoma [81,82].

A series of C6-substituted purine derivatives were designed by Voller *et al.* [83]. The most active compounds, **43** and **44** (Fig. 9), have IC_{50} values of 2.9 and 1.5 μmol/L, respectively. The SAR analysis revealed that the anti-ROCK activity could be further improved by substituting the purine C2 atom or by extension of the purine C6 side chain. Cellular assays show that this compound reduces downstream MLC phosphorylation by inhibiting ROCK and inhibits the invasion of ROCK-dependent melanoma cells into the collagen matrix. Overall, the increase in activity was modest, and all were lower than that of the classical inhibitor fasudil.

3.8. Piperazine derivatives as ROCK inhibitors

Considering the ability of piperazine to form effective hydrogen bonds with ROCK, Li *et al.* introduced phenyl piperazine in the compound. A ROCK-I inhibitor, FPND (**45**) (Fig. 10), was recently reported by Li *et al.* [84]. The structure of **45** consists mainly of naphthalene, triazine and phenylpiperazine. SAR analysis revealed that the fragments of the naphthalene ring are essential for maintaining the activity of 45; phenylpiperazine is also required for antihemorrhagic activity, particularly the fluorine atom of phenylpiperazine, predominantly controlled **45** activity independently. Studies showed **45** interacts with ROCK-I mainly through the following nonpolar links: Val90 and Lys105 with the naphthalene ring and fluorophenyl ring with residues Met153 and Met156. Further studies demonstrate **45** prevents statin-induced cerebral hemorrhage in a zebrafish model through inducing cytoskeletal rearrangement and enhancement of cell–cell junctions in endothelial cells (ECs) *via* ROCK-I and VE-cadherin (VEC) signaling pathways [84–86]. In addition, **45** exhibits very low toxicity in mice through oral administration. Further investigation on the interactions between **45** with ROCK-II and VECs is needed. Ladduwahetty *et al.* [87] designed and synthesized a series of ROCK inhibitors with piperazine core based on SAR and molecular modeling analysis for identifying the small molecules with better central nervous system-penetrant and target specificity for treating the symptoms associated with Huntington's disease (HD). The lead compound **c** (Fig. S8 in Supporting information) showed good potency but poor kinase selectivity [60,63,88]. Fluorine substitution at the 3-position of pyridine greatly improved potency compared to the 2-position substitution. Substitution of the core benzene ring on the lead compound **c** with 2*R*-methylpiperazine resulted in a small increase in kinase activity and a significant increase in cellular potency (Fig. S8). The representative compound **46** (Fig. 10) exhibited good solubility, permeability, and kinome selectivity. The binding kinetics for compound **46** demonstrated a slow dissociation rate (k_{on}: 4.06×10^5 s^{-1}, k_{off}: 1.31×10^{-3} s^{-1}, residence time = 763 s). The relevant *in vitro* absorption, distribution, metabolism and excretion (ADME) assays indicated that incorporating fluorine atom on the methoxy group that on the electron-rich phenyl ring at the positions of *o*-, *m*-, and *p*- decreases the compound stability and leads to high efflux. The presence of the 3-fluoro substituent on the pyridine mitigates the risk of CYP3A4 inhibition compared to the 2-fluoro substituent, and compound **46** inhibited CYP3A4 with an IC_{50} value of 1.1 μmol/L. Comparing the PK parameters of compound **46** given in mice with the dose of 2 mg/kg through intravenous (i.v.) and oral administration revealed it has a high oral bioavailability [87]. Furthermore, compound **46** showed excellent properties of penetrating the blood–brain barrier and showed highest brain area under the concentration *versus* time curve (AUC). Compound **46** dose-dependently leads to an increase in protein kinase B (PKB, also known as AKT) phosphorylation (a distal substrate of the ROCK pathway) and a decrease in MYPT1 phosphorylation. Compound **46** showed a superior profile in all *in vitro* cellular readouts. It has a potent pharmacodynamic effect after oral administration. In the chemoproteomics KiNativ technology (ActivX Biosciences), dose- and time-dependent ROCK-I and ROCK-II target engagement were observed at a 10 mg/kg dose showing equipotency toward each isoform, with a free brain KiNativ ROCK-I and ROCK-II with the IC_{50} values at around 6 nmol/L. Administration of the pi-perazine analogue **46** in the heterozygote Q175DN KI mouse model of HD through chronic dosing (10 mg/kg BID for 90 days) resulted in brain concentrations that were lower than anticipated when compared to a single dose. Notably, neurological index scoring of the mice remained normal at all doses administered.

3.9. Boron derivatives as ROCK inhibitors

In recent years, more and more studies have shown that the boronic acid part of the benzoxaborane compounds serves as the binding hinge to the residue part of various kinases. Dayal *et al.* synthesized a series of 3*H*-pyrazolo[4,3-*f*]quinolone ROCK inhibitors containing boronic acids [89]. Among which, the compound HSD1590 (**47**) (Fig. 10) showed greater than 90% inhibition at the dose of 50 nmol/L, with the IC_{50} values of 1.22 ±

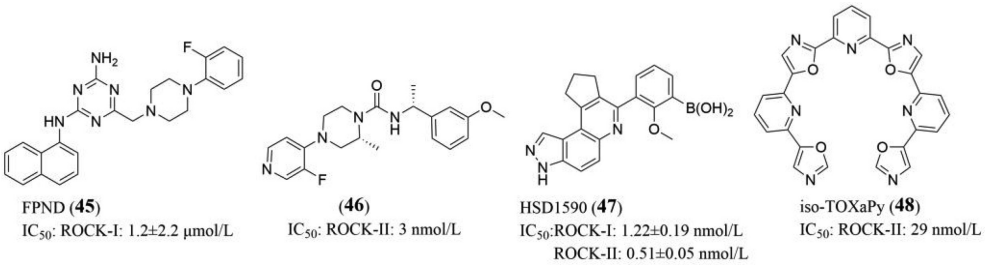

Fig. 10. Piperazine, boron, and ligooxazole and pyridyl oligomeric derivatives as ROCK inhibitors.

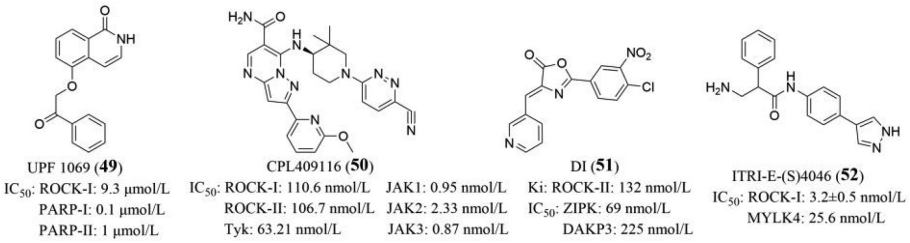

Fig. 11. Bis-functional ROCK inhibitors.

0.19 nmol/L and 0.51 ± 0.05 nmol/L for ROCK-I and ROCK-II, respectively. SAR analysis showed that the compounds containing phenylboronic acids substituted at the 3-position exhibited better ROCK inhibitory activity than furanyl or phenylthio boronic acids, while the introduction of a methoxy at the 2-position in the phenyl group significantly increased the inhibition activity. The *in vitro* assay showed **47** inhibited the migration of breast cancer cell line MDA-MB-231 at 1 μmol/L with low cytotoxicity. Boron derivatives have been less studied as ROCK inhibitors, and the previously discovered boron derivatives have a poor ROCK inhibitory effect. **47** is one of the most effective ROCK inhibitors, but more investigations are needed.

3.10. Ligooxazole/pyridyl oligomeric derivatives as ROCK inhibitors

G-quadruplexes (G4s) are four-stranded nucleic acid secondary structures [90]. Given that G4s are frequently associated with breakpoint regions during DNA replication, telomeric dysfunctions and repression of oncogene expression, G4-binding molecules may have the potential to be developed as one approach for treating cancer [91]. Verga *et al.* identified some oligooxazole/pyridyl oligomeric derivatives as ROCK-II inhibitors in synthesizing compounds that target G4 [92]. The *in vitro* experiments have shown that the oligooxazole/pyridyloligomeric compounds all possess G4 binding activity. Among these compounds, iso-TOXaPy (**48**) (Fig. 10) exhibited excellent ROCK-II inhibitory effects with an IC_{50} value of 29 nmol/L. Further studies revealed that the **48** specifically targets ROCK-II under both *in vitro* conditions and in cells. Besides, the cellular experiment results showed **48** also exhibits high antiproliferative effects on multiple cancer cell lines including glioblastoma, HeLa cells, epidermal cells and melanoma cells. Unlike the common water-soluble ROCK inhibitors, these oligoheteroaryl derivatives have poor water solubility. They are difficult to enter the organism's circulation directly. However, their flexible oligomeric scaffolds adopt multiple conformations that may facilitate intra-organoid circulation and influence their expansion, suggesting their potential applications in antitumor treatment.

3.11. Bis-functional ROCK inhibitors

Currently, developing small molecular bispecific ROCK inhibitors is the hot topic in the field. This type of inhibitor includes ROCK inhibition plus another therapeutically relevant non-kinase target, as simultaneous inhibition of two or more synergistic targets provides better therapeutic efficacy.

Poly(ADP-ribose) polymerase (PARP) inhibitors (PARPi) have therapeutic potential for ovarian cancer, thymic cancer, pancreatic cancer and prostate cancer [93]. Antolín *et al.* screened out the previously published commercial chemical probe UPF 1069 (**49**) (Fig. 11), a 2*H*-isoquinoline 1-one scaffold substituted at position 7 [94,95]. **49** has the IC_{50} values of 0.1 and 1.0 μmol/L for inhibiting PARP1 and PARP2 under *in vitro* conditions, respectively. **49** and hydroxyfasudil have benzamide pharmacodynamic groups in their structures, and both compounds have similar structural properties with micromolar PARP inhibitor CHEMBL1767049 [96,97]. Previous studies demonstrated there are cross-pharmacological properties between ROCK and PARP, and a query of open targets mining revealed that the two protein families share seven diseases areas. The team, therefore, suspected that **49** also has ROCK inhibitory activity and subsequently found that **49** also showed 38% ROCK-I and 20.5% ROCK-II inhibition at 10 μmol/L, with an IC_{50} value of 9.3 μmol/L for ROCK-I. Dual PARP-ROCK inhibitors may play an important role in cancer, DR, AD, cardiovascular disease, skin and skeletal system disorders, and therefore **49** is an excellent lead compound for further study.

The Food and Drug Administration (FDA) has approved three rheumatoid arthritis (RA) indications drugs: baricitinib, tofacitinib and upadacitinib. Early clinical trials have demonstrated the application of Janus kinase (JAK) inhibitors as an effective treatment for a variety of autoimmune diseases [98–100]. Celon Pharma S.A. reported CPL409116 (**50**) (Fig. 11), a potent and selective inhibitor of JAK and ROCK as an alternative therapeutic agent for the systemic lupus erythematosustreatment (SLE) [101]. JAK is a family of non-receptor tyrosine kinases and co-mediates signals from growth factors with tyrosine kinase 2 (Tyk2). Upon activation, JAK leads to downstream phosphorylation of signal transducers and activates the transcription (STATs) of genes associated with the development of SLE symptoms. Since ROCK plays an important role in immune cell regulation and inflammatory disease development, inhibition of ROCK may also be exploited for treating SLE [102,103]. Surprisingly, the ADP-Glo data showed **50** is over 40 times more potent in blocking ROCK activity than fasudil. Besides, **50** also displayed high affinity towards JAK1/2/3 kinases (IC_{50} 0.95/5.36/0.87 nmol/L, respectively) and moderate towards ROCK-I/II kinases (IC_{50}

Table 1
Overview of ROCK inhibitors in clinical trials.

Compound	Therapeutic application	Phase and status	Clinical Trials. gov Identifiers
Belumosudil	Graft-*versus*-host disease; idiopathic pulmonary fibrosis; liver disease; scleroderma	Approved	
	Hepatic impairment	I (Completed)	NCT04166942
	Autoimmune diseases; fibrosis	I (Completed)	NCT03907540
	System; sclerosis; diffuse cutaneous systemic sclerosis	II (Active, not recruiting)	NCT03919799
	Drug–drug interaction; autoimmune diseases; fibrotic disease	I (Completed)	NCT03530995
	Chronic plaque psoriasis	II (Completed)	NCT02852967
	Graft *vs.* host disease	II (Completed)	NCT02841995
	Idiopathic pulmonary fibrosis	II (Completed)	NCT02688647
	Bioavailability	I (Completed)	NCT02557139
	Psoriasis vulgaris	II (Completed)	NCT02317627
	Psoriasis vulgaris	II (Completed)	NCT02106195
	Solid tumor; hepatocellular carcinoma; colorectal cancer; glioma	I (Not yet recruiting)	NCT04550663
Netarsudil	High intraocular pressure; glaucoma	Approved	
PG324[a]	Open angle glaucoma; ocular hypertension	III (Completed)	NCT03284853
	Open angle glaucoma; ocular hypertension	II (Completed)	NCT02057575
CPL409116	Safety and pharmacokinetics CPL409116 in healthy volunteers	I (Completed)	NCT04670757
	Rheumatoid arthritis	II (Recruiting)	NCT05374785

[a] Netarsudil in combination with latanoprost.

110.6/106.7 nmol/L, respectively). This dual inhibitor is competitive but binds to additional enzymes at higher concentrations. For example, Tyk ($IC_{50} = 63.21$ nmol/L). The cellular experiment results showed **50** effectively blocked the proliferation of CD4 T cells and the activation of B cells and reduced the expression of multiple cytokines [including interleukin-1β, 4, 10, 17, 21 and 22, interferon gamma (IFNG) and tumor necrosis factor alpha (TNFα)] by mediating ROCK and JAK. Moreover, the oral administration of 20 mg/kg compound **50** twice a day to SLE mice effectively alleviated SLE-associated organ damage (predominantly in kidneys) and improved the survival rate of SLE mice in a dose-dependent manner. Currently, **50** is going through phase I or II clinical trials and exhibited excellent activity in treating active RA (Table 1).

The (4*Z*)-2-(4-chloro-3-nitrophenyl)-4-(pyridin-3-ylmethylidene)-1,3-oxazol-5-one (DI) (**51**) (Fig. 11), molecule was originally discovered as a potent inhibitor of Zipper-interacting protein kinase (ZIPK) ($IC_{50} = 69$ nmol/L) and death-associated protein kinase 3 (DAPK3) ($IC_{50} = 225$ nmol/L) [104].

AI-Ghabkari *et al.* [104] re-examined the **51** and found that ROCK-II is prominently off-target for **51**. The application of **51** to human coronary artery vascular smooth muscle cells (CASMCs) attenuated myosin regulatory light chains (LC20), Par-4, LIMK and cofilin phosphorylations. However, phosphorylation of cofilin was not significantly reduced with the ZIPK/DAPK-selective inhibitor (HS-38). Cofilin has been identified as a downstream target of ROCK signaling, suggesting that **51** has a ROCK inhibitory effect. Enzyme kinetic experiments determined the potency of compound **51** ($K_i = 132$ nmol/L) toward ROCK-II to be similar to that of Y27632 ($K_i = 140$ nmol/L) and fasudil ($K_i = 158$ nmol/L). Previous studies have shown that administration of compound **51** *in vivo* in spontaneously hypertensive rats effectively reduces blood pressure, reactive oxygen species (ROS) production, and inflammatory responses. **51** also inhibits TNFα-induced inflammatory responses through a ROS-dependent mechanism. All these results suggest that **51** is a promising ROCK/ZIPK/DAPK inhibitor [105].

Chen *et al.* reported a novel, highly specific ROCK-I and MYLK4 inhibitor, ITRI-E-(*S*)4046 (**52**) (Fig. 11) [106]. With strong synergistic inhibition of ROCK-I and MYLK4, **52** reduced IOP in normotensive and hypertensive animal models with minimal hyperemia. Topical application of 0.1% **52** resulted in a peak active drug concentration in plasma at 2 h (3.0 ng/mL), while **52** has a short half-life and disappears within 60 min after topical administration to rabbit eyes. From hepatic microsomal stability studies, **52** gave a mean intrinsic clearance of 8.56 μL min^{-1} mg^{-1} in humans [107]. Further studies are needed to determine whether **52** interferes with other kinases and whether it has cytotoxic effects on ocular tissues.

In a recent patent application, Aerie *et al.* reported synthesizing a series of ROCK and monoamine transporters (MAT) bi-functional inhibitors for targeting glaucoma [108]. The 6-substituted isoquinoline amide scaffold series is structurally similar to netarsudil and may act as rho kinase inhibitors. The chemistry section of the patent exhaustively described the synthesis of a diverse range of compounds prior to their potential applications, with a focus on anti-glaucoma activity. Unfortunately, patents do not report ROCK and MAT inhibition data, such as positive results related to kinase selectivity and hyperemia [109].

3.12. Drug repurposing

Over the past few decades, given the high attrition rates, substantial costs, and slow pace of new drug discovery and development, repurposing drugs approved for the market has emerged as a potential strategy to reduce development costs. For example, thalidomide was initially marketed as a sedative in 1957 and later used to treat erythema nodosum leprosum (ENL) (1964) [110] and multiple myeloma (1999) [111]. Typically, the first step in drug repurposing is the identification of candidate molecules for a given indication (hypothesis generation), which can be subdivided into computational and experimental approaches. Computational methods include signature matching, computational molecular docking, genome-wide association studies, pathway or network mapping, retrospective clinical analysis, and the use of electronic health records. Experimental methods include binding assays to identify target interactions [112]. This approach can also develop ROCK inhibitors by matching the transcriptome signature of fasudil with other drugs. For example, Iorio *et al.* found that fasudil could be applied in amyotrophic lateral sclerosis (ALS) [113–115].

Ansar *et al.* virtually screened 1852 ligands approved by the FDA to dock with binding mode of ROCK (PDB ID: 3NCZ). Conivaptan (**53**) and polydatin (**54**) (Fig. 12) from the FDA-approved Drugbank dataset were potentially repurposable inhibitors targeting ROCK-I. By the same approach, the team also identified WWWF and WWVW as potential and novel tetrapeptide inhibitors targeting the ATP binding domain of ROCK-I. Regrettably, in order to conduct therapeutic studies, it is necessary to experimentally validate these molecules or peptides. However, the authors did not disclose the precise structures and biological activity information of WWVW and WWWF [34].

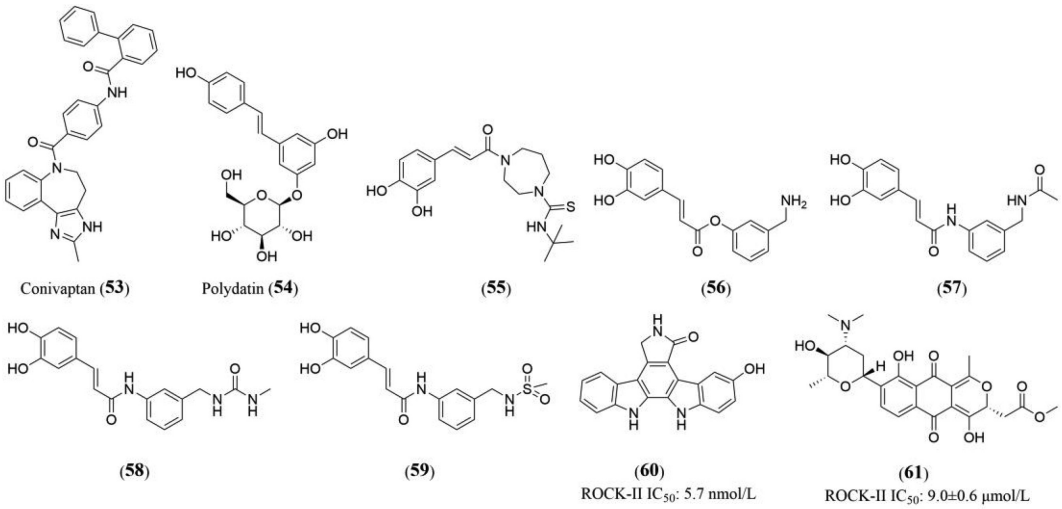

Fig. 12. Structures of ROCK inhibitors discovered from drug repurposing and natural compounds.

Some of the classic drugs with newly identified ROCK inhibitory effects are summarized below. ÖZDEMİR *et al.* found that the FDA-approved anti-type II diabetes drug metformin inhibits ROCK through the connectivity map program. This study further revealed the mechanisms of metformin, which has a guiding significance for the treatment of various pathological conditions involving ROCK, such as asthma, cancer, erectile dysfunction and glaucoma [116]. Recently, Borin *et al.* found that melatonin delays cancer progression not only *via* inhibiting the tumor cells proliferation but also through a direct inhibition of ROCK-I which results in the anti-metastatic effects in the tested cancer cell lines [117]. Nicotinamide is an inhibitor of multiple kinases, and Meng's team recently discovered that it has ROCK inhibitory properties [118]. The *in vitro* experiments results demonstrated that nicotinamide affects the pluripotency and differentiation of human embryonic stem cells. Also, nicotinamide promotes pancreatic progenitor cell differentiation through dual inhibition of ROCK and casein kinases [119]. Discovering more ROCK inhibitors through drug repurposing methods at a lower cost is a feasible research direction.

3.13. Natural compounds as ROCK inhibitors

The extraction of compounds from natural products represents a powerful strategy for the discovery of new bioactive molecules [120–122]. There are a number of research groups that did tremendous work to further optimize the natural origin ROCK inhibitors, and their recent progress has been summarized below.

Arya *et al.* found that three plant constituents: acteoside, martinoside and osmanthuside β6 from *Clerodendrum colebrookianum Walpers*, made critical interactions with the drug targets ROCK-I/II. Specifically, the phenolic hydroxyl group from the aglycone portion of acteoside and osmanthuside β6 was found interact with the hinge region residue Met156/Met157 of ROCK-I/II [123]. Arya *et al.* designed a series of hybrid molecules based on caffeic acid, ferulic acid and *p*-coumaric acid structures (the aglycone portion of the three plant constituents) with the homopiperazine ring of fasudil [124]. Among which, the thiourea analogue **55** (Fig. 12) ($IC_{50} = 25$ μmol/L) showed more than 3-fold anti-proliferative activity than fasudil ($IC_{50} = 87$ μmol/L) in colon cancer cells (SW480). The molecular docking and molecular dynamics simulation results showed compound **55** forms three hydrogen bonds with ROCK-I (Glu154, Met156, Asp202) and ROCK-II (Lys106, Met157, Asp203), respectively. Cellular experiments results showed compound **55** has excellent anti-proliferation and anti-migration activities against tested cancer cell lines [124]. Besides, Arya *et al.* synthesized a series of ROCK inhibitors based on caffeic acid scaffolds. Basic medicinal chemistry rules, coupled with structural insights generated by docking, led to the design of compounds **56**, **57**, **58** and **59** (Fig. 12) were selected as potential ROCK-I inhibitors. To further explore the inhibition mechanisms of the four lead compounds, approaches including Lipinski's rule of five (Ro5), density functional theory (DFT) calculations, molecular docking and molecular dynamics simulations were taken and the results suggest the compounds bind to ROCK-I with a lower binding free energy than fasudil does. However, further cellular experiments are needed to validate the aforementioned mechanisms [125].

Amen *et al.* screened 35 compounds from the total ethanol extract of medicinal mushroom *Ganoderma* (lingzhi), and all compounds showed ROCK inhibitory activities. Further studies revealed that the extract containing lanostane triterpenes exhibit highest ROCK inhibitory activity. Thus, lanostane triterpenes can be potential lead compounds for further investigation as ROCK inhibitors [126].

Liu *et al.* elucidated that six isoquinoline alkaloids of the genus *Lotus* are potential ROCK-I inhibitors. Compared with other alkaloids and fasudil, neoliensinine exhibits a higher ROCK-I binding energy which makes it an irreversible ROCK-I inhibitor [127]. *In vitro* cellular experiment and animal trial results showed that neoliensinine inhibits mesenteric vascular smooth muscle contraction [127,128].

Wang *et al.* isolated nine new indolocarbazoles from marine-derived *Streptomyces* sp. DT-A61. This class of compounds showed significant activity against human prostate PC-3 cancer cells. Among which, the compound **60** (Fig. 12) showed significant inhibitory effects of ROCK-II with an IC_{50} value of 5.7 nmol/L [129]. Similarly, Jiang *et al.* identified four new Medermycin-type naphthoquinones from *Streptomyces*, of which compound **61** (Fig. 12) exhibited moderate inhibition of ROCK-II with an IC_{50} value of 9.0 ± 0.6 μmol/L [130].

Ezzat *et al.* reported the *E. longifolia* aqueous extract inhibits ROCK-II under *in vitro* conditions. The maximum percentage inhibition of ROCK-II by transconiferyl aldehyde isolated from this plant was 82.1% ± 0.63% with an IC_{50} value of 153 ± 14.1 ng/mL, which was better than the IC_{50} value of standard Y-27632 (192 ± 8.37 ng/mL) [131].

Nimgampalle's study revealed that plant extracts, such as quadrangularin, luteolin and laetevirenol, have ROCK-II inhibitory effects [132]. Amen *et al.* found that *C. lacryma-jobi* seeds extracts

Table 2
Peptides reported by Gu and Abbasgholizadeh [24,149].

Peptide	Sequence	Experimental binding affinity K_d (μmol/L)	
		ROCK-I	ROCK-II
IIoI-p1	AMNIPQAIKNILMS	>500	23.60
IoII-p5	TDGWLECIDVIVY	3.90	327.30
Peptide7	ERTYSPSTAVRS	1.458 ± 0.28	5.153 ± 1.15
Peptide22	ERTYSPS	-	-

β-sitosterol, stigmasterol, chlorogenic acid, 2-*O*-β-glucopyranosyl-7-methoxy-2*H*-1,4-benzoxazin-3(4*H*)-one have higher ROCK inhibitory activities compare to the control Y-27632 [133]. In addition, natural extracts such as glycyrrhizin [134], curcumin [135], sodium aescinate [136], catalpol [137], terpinen-4-ol [138], total flavone from *Rhododendron simsii* Planch flower [139,140], *loganin* [141], ferulic acid [142], tetrandrine [143], oxymatrine [144], baicalein [145], sanggenon c [146] and hirudin [147], were found to be potential ROCK inhibitors as well.

3.14. Peptides as ROCK inhibitors

In addition to the tetrapeptides mentioned in the previous section on drug repurposing, other ROCK inhibitory peptides are summarized below. Considering that the dimerization domains (coiled-coil domains) of two ROCK isoforms share relatively low conservation (55%–60%) and ROCK dimerization is a critical biological event in activating the Rho signaling pathway, developing dimerization-disrupting peptides to selectively target the dimerization domains of the two isoforms is also an effective strategy for ROCK inhibitor development [148].

By isolating three helical peptides: H1, H2 and H3 from the kinase dimerization domain, Gu *et al.* found that the ROCK-I H2 and ROCK-II H2 peptides could bind to the active pocket of the kinase dimerization domain [149]. Through hundreds of parallel simulated annealing runs, two peptides were obtained that possess optimal selectivity for ROCK and can effectively inhibit its activity. IoII-p5 (ROCK-I over ROCK-II) and IIoI-p1 (ROCK-I over ROCK-II) were designed to have strong IoII and IIoI selectivity for ROCK-I over ROCK-II (83.9-fold) and for ROCK-II over ROCK-I (> 21.2-fold), respectively (Table 1). Structural modeling results revealed that the non-conserved residues (including T1, D9, V10 and Y13) play a crucial role in defining the peptide selectivity, while conserved residues confer stability to kinase peptide binding [149]. The above results identify the crucial residues of such peptides and their functions, which are important for developing ROCK inhibitors.

Abbasgholizadeh *et al.* screened a phage display library at high levels of ATP (1 mmol/L) and detected peptides that bind to the ROCK N' terminal catalytic domain of ROCK [24]. The investigators identified peptide7, a highly selective allosteric ROCK inhibitory peptide. Considering the long sequence of peptide7, the investigators identified the critical residues of peptide7. They found that tyrosine-serine-proline-serine (YSPS) is the critical amino acid residue that determines the inhibitory properties of the peptide, and obtained peptide22, a highly selective allosteric ROCK inhibitory peptide, with an IC_{50} value of 44.4 μmol/L for ROCK-I (Table 2). In the wire myography assay, peptide22 effectively relaxed the contracted aortic rings, and this effect was in a dose-dependent manner with the maximum inhibitory effect observed at 250 μmol/L. Furthermore, In the presence of 0.1% DMSO, peptide22 was shown to be effective in the corneal neovascularization model. Peptide22 is a very potential ROCK inhibitory peptide. It has shown good activity in tissue and organ assays, but its *in vivo* activity, efficacy, safety and specific mechanisms remain to be investigated. The highlight is that this study reveals that tthese peptides effectively inhibit ROCK, which could guide the development of novel ROCK inhibitory peptides [24]. In the future, peptide drug delivery systems (DDS) capable of binding to peptide inhibitors to enhance their bioavailability may play a significant role in the further development of ROCK inhibitors [150].

4. Conclusion and perspective

ROCK is an attractive target for various pathological conditions as a critical mediator of the cellular response to environmental signals. ROCK is distributed throughout the body, with ROCK-I mainly in the lung, liver, testis, blood and immune system, and ROCK-II more significantly expressed in the brain, heart and smooth muscle cells. ROCK signaling is involved in various processes, such as metastasis, invasion, tumor growth and angiogenesis in various cancers. ROCK also plays a vital role in regulating cellular morphology and cardiovascular function. Therefore, research targeting ROCK is rapidly developing in treating various diseases such as cancer, neurological diseases, inflammation, cardiovascular diseases and glaucoma. Although several ROCK inhibitors have been developed, only four have been approved for clinical application, including fasudil, ripasudil, netarsudil and belumosudil. In this review, we summarized more than 60 ROCK inhibitors with different chemical families, including isoquinoline, pyridine, indazole, pyrimidine, pyrroloxypyridine, pyrazole, thieno[2,3-*d*]pyrimidin-4(3*H*)-one, benzothiophene, 4-chromanone, benzimidazole, naphthalene, purine, boron, ligooxazole/pyridyl oligomeric derivatives and other small molecule inhibitors. These small molecule inhibitors tend to exhibit more potent ROCK inhibition. However, the development of these compounds is still in a relatively early stage, and most of the ROCK inhibitors reported to be effective are ATP-competitive inhibitors. The selectivity of these compounds may be limited. Due to the pervasive distribution of ROCK in the human body, its inhibition may cause some adverse reactions caused by the off-target effects observed in both preclinical studies and clinical applications, such as renal insufficiency, intestinal obstruction and systemic hypotension. Therefore, the screening and design of ROCK-targeted drugs require more consideration of their protein structure, and the selectivity, inhibitory efficacy and safety must be balanced. Scientists have observed that DDS possess the capability to administer medications for diverse ailments, surmounting issues related to drug inefficacy and delivery hurdles. The potential of DDS is not confined to a particular disease but can be employed for a multitude of maladies. For instance, nanomaterials and liposomes as biological drug carriers have shown promise in delivering drugs for cancer and Alzheimer's disease treatment [151–154]. Thus, the development of new DDS could potentially optimize the pharmaceutical profiles of ROCK inhibitors [155–158], with articles reporting VA-coupled liposomal ROCK inhibitors that target hepatic stellate cells to inhibit hepatic fibrosis without causing systemic side effects [156,159]. In addition, several studies reported the selection of macrocyclic host molecules or peptides as molecular carriers for ROCK inhibitors, which improved drug stability and bioavailability [160,161]. The potential approaches include developing bioreductive prodrugs and photo-controllable drugs [162,163]. The development of stable and controllable ROCK inhibitors is the future direction of solving the adverse reaction problem.

In addition to the development of novel small molecule inhibitors for ROCK, the identification of ROCK inhibitors from existing marketed drugs holds promise for the discovery of multi-target inhibitors with enhanced efficacy. For example, compound **50**, a multi-target inhibitor of JAK and ROCK, has been approved for phase II clinical trials in active RA. Multi-target ROCK inhibitors have a higher potential to simultaneously inhibit two or more multiple targets than single-target ROCK inhibitors. Further-

more, the natural extract derivatives of ROCK inhibitors have been reported and are in the early stages of preclinical studies. Further biophysical studies of natural ROCK inhibitors and derivatives are warranted, which may contribute to developing effective ROCK inhibitors in the future. In addition to the standard small molecule compounds as ROCK inhibitors, we noted that peptide-based agents that target active pockets of the kinase dimerization domain might be the basis for further work.

The recent years have been characterized by an impressive surge in developmental activities in the field of ROCK inhibitors focusing on improved target selectivity and refined pharmacological properties to reduce unwanted side effects. This review discusses some important SAR and ROCK inhibitors binding modes, design approaches, and clinical studies. By utilizing these structures and drug design approaches, the development of more effective and selective ROCK inhibitors could provide a stronger scientific basis for treating various diseases.

Declaration of competing interest

The authors declare that they have no known competing financial interests or personal relationships that could have appeared to influence the work reported in this paper.

Acknowledgments

This work is supported by the National Natural Science Foundation of China (Nos. 82073311 and 81973866), Natural Science Foundation of Sichuan Province (No. 2022JDTD0025), Science and Technology Research Project of Sichuan Traditional Chinese Medicine Administration (No. 2021ZD016).

Supplementary materials

Supplementary material associated with this article can be found, in the online version, at doi:10.1016/j.cclet.2023.108336.

References

[1] J. Hu, P. Zhu, Y. Li, Y. Chen, Chin. Chem. Lett. 29 (2018) 1043–1050.
[2] J. Shi, L. Wei, Arch. Immunol. Ther. Exp. 70 (2022) 4.
[3] T. Ushijima, N. Fujimoto, S. Matsuyama, et al., J. Biol. Chem. 293 (2018) 148–162.
[4] N. Karimi, F. Bayram Catak, E. Arslan, et al., Int. Immunopharmacol. 113 (2022) 109445.
[5] D.R. Thal, S.O. Tome, Brain Res. Bull. 190 (2022) 204–217.
[6] C. Hu, H. Zhou, Y. Liu, et al., Int. J. Oncol. 55 (2019) 833–844.
[7] Y. Hiroi, K. Noma, H.H. Kim, et al., Circ. J. 82 (2018) 1195–1204.
[8] L. Julian, M.F. Olson, Small GTPases 5 (2014) e29846.
[9] W. Chen, M.S. Nyuydzefe, J.M. Weiss, et al., Sci. Rep. 8 (2018) 16636.
[10] N. Zhou, J.J. Lee, S. Stoll, et al., Cell. Physiol. Biochem. 44 (2017) 701–715.
[11] E. Berrino, C.T. Supuran, Expert Opin. Ther. Pat. 29 (2019) 817–827.
[12] C. Vennin, V.T. Chin, S.C. Warren, et al., Sci. Transl. Med. 9 (2017) eaai8504.
[13] L. Deng, G. Li, R. Li, et al., Cancer Biol. Ther. 9 (2010) 875–884.
[14] I. Hinsenkamp, S. Schulz, M. Roscher, et al., Neoplasia 18 (2016) 500–511.
[15] J.M. Thompson, Q.H. Nguyen, M. Singh, et al., Oncogene 36 (2017) 1080–1089.
[16] Y. Xia, X. Cai, J. Fan, et al., Anticancer Drugs 28 (2017) 514–521.
[17] Z.H. Wang, D. Zhu, S. Xie, et al., J. Cardiovasc. Pharmacol. 70 (2017) 102–109.
[18] N.T. Abdali, A.H. Yaseen, E. Said, T.M. Ibrahim, Naunyn. Schmiedebergs Arch. Pharmacol. 390 (2017) 409–422.
[19] T.L. Montagnoli, J.S. da Silva, S.Z. Sudo, et al., Cells 10 (2021) 1648.
[20] D. Xueyang, M. Zhanqiang, M. Chunhua, H. Kun, Oncotarget 7 (2016) 78764–78772.
[21] L. Qi, Y.G. Tang, L. Wang, et al., J. Neurol. Sci. 370 (2016) 21–26.
[22] J.L. Labandeira-Garcia, A.I. Rodriguez-Perez, B. Villar-Cheda, et al., Neuroscientist 21 (2015) 616–629.
[23] J. Han, Y. Zhao, Y. Zhang, et al., Front. Pharmacol. 9 (2018) 87.
[24] R. Abbasgholizadeh, H. Zhang, J.W. Craft Jr., et al., Exp. Biol. Med. 244 (2019) 940–951.
[25] L. Song, C. Zhu, W. Zheng, et al., Comput. Biol. Chem. 87 (2020) 107314.
[26] S.P. Davies, H. Reddy, M. Caivano, P. Cohen, Biochem. J. 351 (2000) 95–105.
[27] Y. Feng, P.V. LoGrasso, O. Defert, R. Li, J. Med. Chem. 59 (2016) 2269–2300.
[28] T. Landry, D. Shookster, H. Huang, Front. Endocrinol. 11 (2020) 622581.
[29] L. Huang, F. Dai, L. Tang, et al., Cell. Physiol. Biochem. 49 (2018) 565–577.
[30] J. Du, J. Guo, D. Kang, et al., Chin. Chem. Lett. 31 (2020) 1695–1708.
[31] S. Ghosh, S. Keretsu, S.J. Cho, PeerJ 9 (2021) e11951.
[32] B. Bayel Secinti, G. Tatar, T. Taskin Tok, J. Biomol. Struct. Dyn. 37 (2019) 2457–2463.
[33] H. Chen, S. Li, Y. Hu, et al., Comb. Chem. High Throughput Screen. 19 (2016) 36–50.
[34] S. Ansar, U. Vetrivel, J. Biomol. Struct. Dyn. 40 (2022) 7450–7468.
[35] A.A. Sadybekov, A.V. Sadybekov, Y. Liu, et al., Nature 601 (2022) 452–459.
[36] J.C. Koch, L. Tatenhorst, A.E. Roser, et al., Pharmacol. Ther. 189 (2018) 1–21.
[37] C.M. Chong, M.T. Kou, P. Pan, et al., Mol. Biosyst. 12 (2016) 2713–2721.
[38] M. Rosen Kenneth, D. Abbinanti Matthew, J. Ruschel, et al., BioAxone BioSciences Inc. Patent, US2020199105 (A1), 2020.
[39] L. McKerracher, R. Shenkar, M. Abbinanti, et al., Transl. Stroke Res. 11 (2020) 365–376.
[40] J. Liang, M. Tang, L. Wang, et al., Chem. Biol. Drug Des. 98 (2021) 1065–1078.
[41] C.M. Avila, A.B. Lopes, A.S. Goncalves, et al., Eur. J. Med. Chem. 46 (2011) 1245–1253.
[42] R.G. Oliveira, F.S. Guerra, C.D.S. Mermelstein, et al., J. Enzyme Inhib. Med. Chem. 33 (2018) 1181–1193.
[43] M. Uehata, T. Ishizaki, H. Satoh, et al., Nature 389 (1997) 990–994.
[44] M. Arita, T. Saito, H. Okuda, et al., Yoshitomi Pharmaceutical Industries Ltd., Patent, US19940204211, 1992.
[45] M. Dietrich, H.P. Hartung, P. Albrecht, Neurol. Neuroimmunol. Neuroinflamm. 8 (2021) e976.
[46] S. Li, D. Wei, Z. Mao, et al., Bioorg. Chem. 73 (2017) 63–75.
[47] Y. Yao, R. Li, X. Liu, et al., Molecules 22 (2017) 1766.
[48] L. Gong, J. Peng, L. Fang, et al., Molecules 17 (2012) 5935–5944.
[49] T.Y. Yuan, Y.C. Chen, H.F. Zhang, et al., Acta Pharmacol. Sin. 37 (2016) 604–616.
[50] A.D. Hobson, R.A. Judge, A.L. Aguirre, et al., J. Med. Chem. 61 (2018) 11074–11100.
[51] Z. Hu, C. Wang, D. Sitkoff, et al., Bioorg. Med. Chem. Lett. 30 (2020) 127474.
[52] Y. Sun, Y. Li, Z. Miao, et al., Bioorg. Med. Chem. Lett. 45 (2021) 128138.
[53] H. Gao, C. Marhefka, M.D. Jacobs, et al., Bioorg. Med. Chem. Lett. 28 (2018) 2616–2621.
[54] U.K. Bandarage, J. Cao, J.H. Come, et al., Bioorg. Med. Chem. Lett. 28 (2018) 2622–2626.
[55] U.K. Bandarage, J. Court, H. Gao, et al., Bioorg. Med. Chem. Lett. 33 (2021) 127721.
[56] S. Ma, L. Wang, B. Ouyang, et al., Bioorg. Med. Chem. 28 (2020) 115683.
[57] L. Wang, B. Ouyang, M. Fan, et al., Iran. J. Pharm. Res. 20 (2021) 121–131.
[58] L. Wang, J. Qi, M. Fan, L. Yao, Chem. Biol. Drug Des. 98 (2021) 969–978.
[59] R. Pireddu, K.D. Forinash, N.N. Sun, et al., MedChemComm 3 (2012) 699–709.
[60] Y. Feng, Y. Yin, A. Weiser, et al., J. Med. Chem. 51 (2008) 6642–6645.
[61] Y. Feng, P. Lograsso, T. Bannister, et al., Patent, WO2008US13844, 2009.
[62] J. Pan, Y. Yin, L. Zhao, Y. Feng, Bioorg. Med. Chem. 27 (2019) 1382–1390.
[63] J. Green, J. Cao, U.K. Bandarage, et al., J. Med. Chem. 58 (2015) 5028–5037.
[64] Z. Hu, C. Wang, P.W. Glunz, et al., Bioorg. Med. Chem. Lett. 30 (2020) 127495.
[65] Z. Miao, Y.M. Sun, L.Y. Zhao, et al., Bioorg. Med. Chem. Lett. 30 (2020) 126966.
[66] Y. Yin, L. Lin, C. Ruiz, et al., Bioorg. Med. Chem. Lett. 19 (2009) 6686–6690.
[67] R.A. Judge, A. Vasudevan, V.E. Scott, et al., ChemBioChem 19 (2018) 613–621.
[68] E.H. Sessions, Y. Yin, T.D. Bannister, et al., Bioorg. Med. Chem. Lett. 18 (2008) 6390–6393.
[69] Y. Feng, T. Chen Yen, H. Sessions, et al., Patent, WO2011050245 (A1), 2011.
[70] M.A. Delong, J. Sturdivant, S.M. Royalty, et al., Invest. Ophthalmol. Vis. Sci. 50 (2009) 4058.
[71] M.A. deLong, J. Yingling, C.W. Lin, et al., Invest. Ophthalmol. Vis. Sci. 53 (2012) 3867.
[72] J.M. Sturdivant, S.M. Royalty, C.W. Lin, et al., Bioorg. Med. Chem. Lett. 26 (2016) 2475–2480.
[73] S.M. Hoy, Drugs 78 (2018) 389–396.
[74] C.R. Hsu, Y.H. Chen, C.P. Liu, et al., Invest. Ophthalmol. Vis. Sci. 60 (2019) 624–633.
[75] C.M. Tu, C.P. Liu, C.H. Chen, et al., Invest. Ophthalmol. Vis. Sci. 60 (2019) 3768.
[76] S. Kesar, S. Paliwal, P. Mishra, et al., ACS Med. Chem. Lett. 11 (2020) 1694–1703.
[77] D. Domokos, F. Fulop, G. Falkay, R. Gaspar, Bioorg. Med. Chem. Lett. 28 (2018) 466–469.
[78] L. Zhao, Y. Li, Y. Wang, et al., J. Med. Chem. 62 (2019) 10691–10710.
[79] K.S. Oh, B.K. Oh, C.H. Park, et al., Eur. J. Pharmacol. 702 (2013) 218–226.
[80] V. Abbhi, L. Saini, S. Mishra, et al., Bioorg. Med. Chem. 25 (2017) 6071–6085.
[81] E. Oshida, Y. Matsumoto, K. Arai, Clin. Ophthalmol. 4 (2010) 653–660.
[82] A. Izzotti, A. Bagnis, S.C. Sacca, Mutat. Res. 612 (2006) 105–114.
[83] J. Voller, L. Zahajska, L. Plihalova, et al., Bioorg. Chem. 90 (2019) 103005.
[84] S. Li, N. Ai, M. Shen, et al., Cell Death Dis 3 (2017) 17051.
[85] T. Skaria, E. Bachli, G. Schoedon, Cell Adhes. Migr. 11 (2017) 24–38.
[86] M. Corada, M. Mariotti, G. Thurston, et al., Proc. Natl. Acad. Sci. U. S. A. 96 (1999) 9815–9820.
[87] T. Ladduwahetty, M.R. Lee, M.C. Maillard, et al., J. Med. Chem. 65 (2022) 9819–9845.
[88] Y.D. Zhao, L. Cai, M.K. Mirza, et al., Am. J. Pathol. 180 (2012) 2268–2275.
[89] N. Dayal, C.G. Mikek, D. Hernandez, et al., Eur. J. Med. Chem. 180 (2019) 449–456.
[90] W. Liu, Y. Xu, X. Li, et al., Chin. Chem. Lett. 32 (2021) 2322–2326.
[91] S. Neidle, J. Med. Chem. 59 (2016) 5987–6011.
[92] D. Verga, C.H. N'Guyen, M. Dakir, et al., J. Med. Chem. 61 (2018) 10502–10518.
[93] C.J. Lord, A. Ashworth, Science 355 (2017) 1152–1158.
[94] A.A. Antolin, J. Mestres, ACS Omega 3 (2018) 12707–12712.

[95] R. Pellicciari, E. Camaioni, G. Costantino, et al., ChemMedChem 3 (2008) 914–923.
[96] H. Chen, Y. Lin, M. Han, et al., J. Pharm. Biomed. Anal. 52 (2010) 242–248.
[97] A. Gaulton, A. Hersey, M. Nowotka, et al., Nucleic Acids Res. 45 (2017) D945–D954.
[98] J.J. O'Shea, D.M. Schwartz, A.V. Villarino, et al., Annu. Rev. Med. 66 (2015) 311–328.
[99] D.M. Schwartz, Y. Kanno, A. Villarino, et al., Nat. Rev. Drug Discov. 17 (2017) 78.
[100] L.M. Mathias, W. Stohl, Expert Opin. Ther. Targets 24 (2020) 1283–1302.
[101] M. Dulak-Lis, A. Bujak, K. Gala, et al., J. Pharmacol. Sci. 145 (2021) 340–348.
[102] R.A. Stirzaker, P.S. Biswas, S. Gupta, et al., Lupus 21 (2012) 656–661.
[103] P.S. Biswas, S. Gupta, E. Chang, et al., J. Clin. Invest. 120 (2010) 3280–3295.
[104] M. Okamoto, K. Takayama, T. Shimizu, et al., Bioorg. Med. Chem. 18 (2010) 2728–2734.
[105] T. Usui, M. Okada, Y. Hara, H. Yamawaki, Hypertension 60 (2012) 1031–1039.
[106] Y.H. Chen, W.Y. Lin, Y.C. Huang, et al., Invest. Ophthalmol. Vis. Sci. 62 (2021) 12.
[107] H. Alrabiah, A.A. Kadi, M.W. Attwa, G.A.E. Mostafa, Chem. Cent. J. 12 (2018) 47.
[108] A. Bonardi, C.T. Supuran, Expert Opin. Ther. Pat. 29 (2019) 753–759.
[109] A. Delong Mitchell, M. Sturdivant Jill, M. Royalty Susan, Aerie Pharmaceuticals Inc., Patent, US2018244666A1, 2018.
[110] T.T. Ashburn, K.B. Thor, Nat. Rev. Drug Discov. 3 (2004) 673–683.
[111] S. Singhal, J. Mehta, R. Desikan, et al., N. Engl. J. Med. 341 (1999) 1565–1571.
[112] S. Pushpakom, F. Iorio, P.A. Eyers, et al., Nat. Rev. Drug Discov. 18 (2019) 41–58.
[113] F. Iorio, R. Bosotti, E. Scacheri, et al., Proc. Natl. Acad. Sci. U. S. A. 107 (2010) 14621–14626.
[114] R. Gunther, A. Balck, J.C. Koch, et al., Front. Pharmacol. 8 (2017) 17.
[115] L. Tonges, R. Gunther, M. Suhr, et al., Glia 62 (2014) 217–232.
[116] A. OzdemIr, M. Ark, Turk. J. Biol. 45 (2021) 35–45.
[117] T.F. Borin, A.S. Arbab, G.B. Gelaleti, et al., J. Pineal Res. 60 (2016) 3–15.
[118] Y. Meng, Z. Ren, F. Xu, et al., Stem Cell Rep 11 (2018) 1347–1356.
[119] Y. Zhang, J. Xu, Z. Ren, et al., Stem Cell Res. Ther. 12 (2021) 1–12.
[120] C. Long, W.C. Luo, H.Y. Zhou, et al., Chin. Chem. Lett. 27 (2016) 247–250.
[121] C.L. Xie, D. Zhang, K.Q. Guo, et al., Chin. Chem. Lett. 33 (2022) 2057–2059.
[122] H. Wang, X. Bai, Y. Huang, et al., Chin. Chem. Lett. 34 (2023) 107671.
[123] H. Arya, S.B. Syed, S.S. Singh, et al., Interdiscip. Sci. Comput. Life Sci. 10 (2018) 792–804.
[124] H. Arya, C.S. Yadav, S.Y. Lin, et al., J. Biomol. Struct. Dyn. 38 (2020) 3563–3577.
[125] H. Arya, M.S. Coumar, J. Mol. Model. 26 (2020) 249.
[126] Y. Amen, Q. Zhu, H.B. Tran, et al., J. Nat. Med. 71 (2017) 380–388.
[127] J. Liu, Y. Lu, G. Li, et al., J. Biomol. Struct. Dyn. 39 (2021) 379–394.
[128] G.M. Yang, J. Sun, Y. Pan, et al., Fitoterapia 124 (2018) 58–65.
[129] J.N. Wang, H.J. Zhang, J.Q. Li, et al., J. Nat. Prod. 81 (2018) 949–956.
[130] Y.J. Jiang, D.S. Zhang, H.J. Zhang, et al., J. Nat. Prod. 81 (2018) 2120–2124.
[131] S.M. Ezzat, M.M. Okba, M.I. Ezzat, et al., Evid. Based Complement. Alternat. Med. 2019 (2019) 4341592.
[132] M. Nimgampalle, H.N. Banavath, H. Chakravarthy, et al., J. Biomol. Struct. Dyn. 38 (2020) 4669–4686.
[133] Y. Amen, Q. Zhu, H.B. Tran, et al., Nat. Prod. Res. 32 (2018) 1955–1959.
[134] Z. Xu, Z. Hu, H. Xu, et al., Exp. Cell Res. 411 (2022) 113008.
[135] Y. Zhou, P.J. Little, S. Xu, D. Kamato, Molecules 26 (2021) 2320.
[136] W. Liu, F. Qin, F. Wu, et al., Phytomedicine 69 (2020) 153193.
[137] A. Shu, Q. Du, J. Chen, et al., Chem. Biol. Interact. 348 (2021) 109625.
[138] W. Cao, R. Tian, R. Pan, et al., Bioengineered 13 (2022) 8643–8656.
[139] X. Cheng, J. Zhang, Z. Chen, Evid. Based Complement. Alternat. Med. 2017 (2017) 5389272.
[140] X.Q. Sun, S. Chen, L.F. Wang, Z.W. Chen, J. Pharm. Pharmacol. 70 (2018) 1713–1722.
[141] Y.T. Tseng, W.J. Lin, W.H. Chang, Y.C. Lo, Phytother. Res. 33 (2019) 690–701.
[142] Z. Wei, Y. Xue, Y. Xue, et al., J. Pharmacol. Sci. 147 (2021) 72–80.
[143] J. Yu, C. Zhu, J. Yin, et al., Drug Des. Devel. Ther. 14 (2020) 361–370.
[144] Y. Wang, Z. Shou, H. Fan, et al., Biosci. Rep. 39 (2019) BSR20182297.
[145] Z. Zhang, L. Nong, M. Chen, et al., Acta Biochim. Biophys. Sin. 52 (2020) 1007–1015.
[146] Y. Zhao, J. Xu, Inflammation 43 (2020) 1476–1487.
[147] J. Chen, W. Shi, Y. Xu, et al., Drug Des. Devel. Ther. 82 (2021) 553–561.
[148] X. Wang, D. Hou, W. Dai, et al., Mol. Inf. 35 (2016) 262–267.
[149] Z. Gu, T. Yan, F. Yan, J. Mol. Recognit. 33 (2020) e2835.
[150] S. Zhao, J. Li, F. Wang, et al., Chin. Chem. Lett. 31 (2020) 1147–1152.
[151] Q. Zhu, M. Saeed, R. Song, et al., Chin. Chem. Lett. 31 (2020) 1051–1059.
[152] H. Zeng, Y. Qi, Z. Zhang, et al., Chin. Chem. Lett. 32 (2021) 1857–1868.
[153] K. Thapa Magar, G.F. Boafo, X. Li, et al., Chin. Chem. Lett. 33 (2022) 587–596.
[154] P. Wang, Y. Wang, P. Li, et al., Chin. Chem. Lett. 34 (2023) 107691.
[155] N.D. Sheybani, H. Yang, Chin. Chem. Lett. 28 (2017) 1817–1821.
[156] H. Zhu, J. Yu, J. Ye, et al., Chin. Chem. Lett. 34 (2023) 107648.
[157] R. Liu, C. Luo, Z. Pang, et al., Chin. Chem. Lett. 34 (2023) 107518.
[158] Y. Gao, Y. Gao, Y. Ding, et al., Chin. Chem. Lett. 32 (2021) 949–953.
[159] S. Okimoto, S. Kuroda, H. Tashiro, et al., Hepatol. Res. 49 (2019) 663–675.
[160] S. Klein, F. Frohn, F. Magdaleno, et al., Sci. Rep. 9 (2019) 2256.
[161] H. Yin, L. Chen, B. Yang, et al., Org. Biomol. Chem. 15 (2017) 4336–4343.
[162] T.A. Al-Hilal, M.A. Hossain, A. Alobaida, et al., J. Control. Release 334 (2021) 237–247.
[163] K. Matsuo, S. Thayyil, M. Kawaguchi, et al., Chem. Commun. 57 (2021) 12500–12503.